

An *In vitro* Study of Bacterial Leakage of a Novel Implant Abutment Interface

Dr. Salma Mohamed Khalifa Kabbashi

Student number: 3619347



A mini-thesis submitted in partial fulfilment of the requirements for the degree of Master of Science in Dental Science in Periodontology at the Department of Oral Medicine and Periodontology, University of the Western Cape.

Supervisor: Dr. M T Peck

Co-supervisor: Mr. Ernest Maboza

<http://etd.uwc.ac.za/>

An *In vitro* Study of Bacterial Leakage of a Novel Implant Abutment Interface

Dr. Salma Mohamed Khalifa Kabbashi

KEYWORDS

Dental implant

Implant-abutment interface

Bacterial leakage

Internal connection

Morse taper

GM connection

CM connection



UNIVERSITY *of the*
WESTERN CAPE

ABSTRACT

An *In vitro* Study of Bacterial Leakage of a Novel Implant Abutment Interface

Dr. Salma Mohamed Khalifa Kabbashi

Master of Science in Dental science in Periodontology, Department of Oral Medicine and Periodontology, The University of the Western Cape.

Background: The two-stage implant system has proven to be a successful technique in replacing missing teeth (Nascimento *et al.*, 2008). Nevertheless, the presence of micro-gaps that could entrap microbes at the implant-abutment interface (IAI) is unavoidable. This microbial leakage has been considered as one of the causes of peri-implant infection and bone loss (Scarano *et al.*, 2005). Several companies have attempted to manufacture an implant with a connection design that provides hermetic sealing against bacterial leakage. Studies indicated that implants with internal connection, in particular the conical (Morse taper) design, have better sealing capacity in the implant abutment interface than the external design (Koutouzis *et al.*, 2011, Jaworski *et al.*, 2012). An internal conical implant system with a novel connection design, known as the Grand Morse (GM) connection, is reported to offer secure connection against micro-leakage (Neodent[®] Implant Systems Inc., 2018).

Aims: The aim of this study was to test the sealing ability against bacterial leakage in the implant-abutment interface provided by an implant with a novel deep internal conical (GM) connection design.

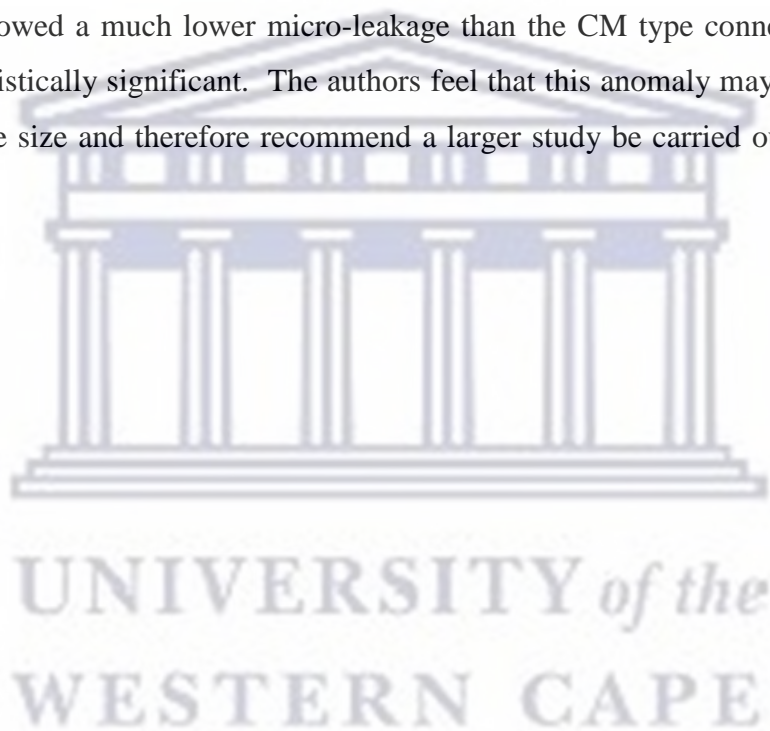
Material and Methods: A total of 20 implants (10 implants per group) were tested in this investigation. Group 1 was composed of implants with a GM connection design, while group 2 had a Cone Morse (CM) connection design. Both groups were injected with 0.05 ml of sterile BHI inside each implant well, then re-connected and subjected to *Streptococcus sanguinis* (10^8 colony forming units/mL) broth in a tube for 48 hours at 37°C 5% CO₂. The assemblies were disconnected and sampled with sterile paper points for bacterial contamination. The paper points were immersed in sterile BHI and cultured on labelled agar plates. After 24 hours, the agar plates were collected and examined for bacterial growth and confirmed by Gram's staining as *Streptococcus sanguinis*. Thereafter, two of the implant assemblies from the positive samples in each group were randomly selected and subjected to SEM analysis for measuring the IAI micro-gap in 12 random points at the interface. Finally,

one of the samples subjected to SEM analysis was chosen from each group for micro CT scanning to measure the depth of the IAI at different equidistant points.

Results: The results showed higher bacterial leakage in CM connection assemblies compared to GM connection but with no statistical differences (Chi square test, $p= 0.175$). For the SEM analysis, the mean values of the micro-gap width were higher in GM connection than CM connection assemblies with a significant statistical difference (independent t-test, $p= 0.00$). For the micro CT scanning, the mean length was higher in the CM group than in the GM group with a statistically significant difference noted (independent t-test, $p= 0.049$).

Conclusion: The current study reported the lack of hermetic sealing against microbial leakage for both IAI type connections. Although the GM type connection showed a larger IAI micro-gap, it showed a much lower micro-leakage than the CM type connection. However, this was not statistically significant. The authors feel that this anomaly may be explained by the small sample size and therefore recommend a larger study be carried out to confirm the current results.

October 2019



DECLARATION

I hereby declare that *An In vitro Study of Bacterial Leakage of a Novel Implant Abutment Interface* is my own work, that it has not been submitted for any degree or examination at any other university, and that all the sources I have used or quoted have been indicated and acknowledged by complete references.

Dr. Salma Mohamed Khalifa Kabbashi

October 2019



ACKNOWLEDGEMENTS

I would like to acknowledge my deep gratitude to my supervisor, Dr. M T Peck, for his support, commitment and encouragement throughout the course of my study. In addition I would also like to thank my co-supervisor, Mr. Ernest Maboza, for his patience and assistance during my research. The completion of this work could not have been achieved without your precious guidance.



DEDICATION

To the love of my life, Hisham, I can't imagine how my life would be without you. Thank you for always being there for me.

To my two little angels and the one on the way, I love you all so much and I am so blessed to have you.



UNIVERSITY *of the*
WESTERN CAPE

TABLE OF CONTENTS

TITLE PAGE.....	i
KEYWORDS.....	ii
ABSTRACT.....	iii-iv
DECLARATION.....	v
ACKNOWLEDGEMENTS	vi
DEDICATION	vii
TABLE OF CONTENTS	viii-ix
LIST OF TABLES	x
LIST OF FIGURES	xi
LIST OF ABBREVIATIONS	xii
CHAPTER 1: INTRODUCTION	1
CHAPTER 2: LITERATURE REVIEW	2
2.1 Background	2
2.2 Types of connection design	2-4
2.2.1 External hexagon connection design	4-6
2.2.2 Internal connection designs	7-10
2.3 A Novel Implant Connection	11-13
2.4 The Rationale of the Study	13
CHAPTER 3: AIMS AND OBJECTIVES	14
3.1 Aim	14
3.2 Objectives	14
CHAPTER 4: MATERIALS AND METHODS	15
4.1 Study design	15
4.2 Sample size	15-17
4.3 Methodology	18
4.3.1 Bacterial culture preparation	18
4.3.2 Bacterial challenge	18-19
4.3.3 Scanning electron microscopy	19-20
4.3.4 Micro Computer tomography (CT) scanning	20-21
4.4 Data collection and analysis	22
CHAPTER 5: RESULTS	23
5.1 Bacterial challenge	22-25

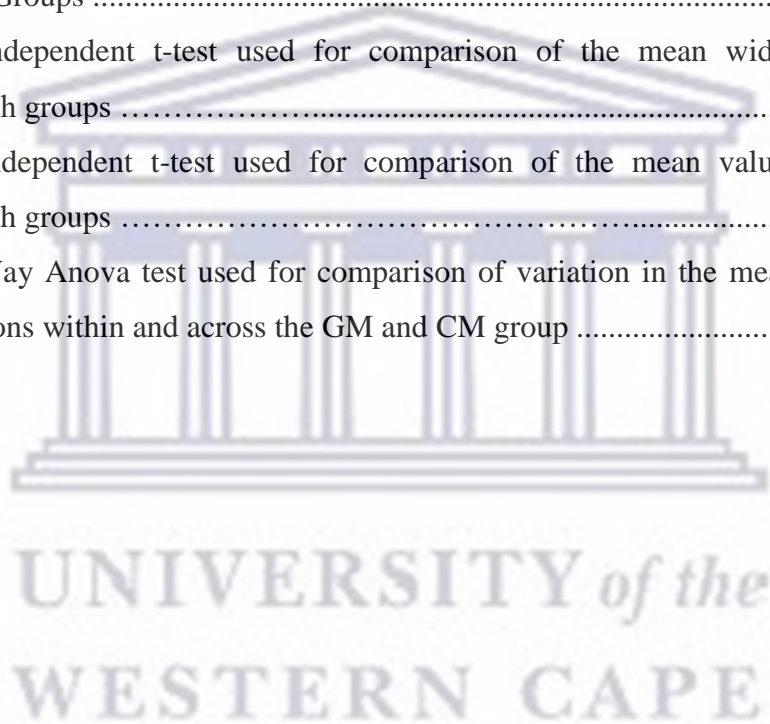
5.2	Scanning electron microscopy	26-30
5.3	Micro Computer tomography (CT) scanning	30-33
	CHAPTER 6: DISCUSSION	34-36
	CHAPTER 7: LIMITATION	37-40
	CHAPTER 8: CONCLUSION	41
	REFERENCES	42-46
	APPENDIXES	47-57



UNIVERSITY *of the*
WESTERN CAPE

LIST OF TABLES

Table 1: Previous work of <i>in vitro</i> clinical studies using an external hexagon connection design	4
Table 2: Comparative <i>in vitro</i> clinical studies between the external hexagon and different internal connection designs.....	6
Table 3: <i>In vitro</i> clinical studies using different internal connection designs	8
Table 4: Characteristics of GM connection design, Neodent® Implant Systems Inc.	13
Table 5: Characteristics of the implants included in the current study	17
Table 6: The Chi-Square Tests used for comparison of presence or absence of bacterial leakage in both Groups	27
Table 7: An independent t-test used for comparison of the mean width and standard deviations in both groups	31
Table 8: An independent t-test used for comparison of the mean values and standard deviations in both groups	34
Table 9: One Way Anova test used for comparison of variation in the means of depth and standard deviations within and across the GM and CM group	35



LIST OF FIGURES

Figure 1: Example of external connection designs	3
Figure 2: Examples of internal connection designs.....	3
Figure 3: A- The novel GM implant connection. B- Dimensions of the GM connection in Helix GM implants	12
Figure 4: A- Helix GM implant fixture. B-Drive CM implant fixture	14
Figure 5: Samples of the GM group labelled agar plates	23
Figure 6: Samples of the CM group labelled agar plates	24
Figure 7: Graph illustrating the bacterial leakage in the GM and CM groups	25
Figure 8: Measurement of the interface of the external entrance, in micrometer, at random points in implant assemblies from the GM group using a SEM image	27
Figure 9: Measurement of the interface of the external entrance, in micrometer, at random points in implant assemblies from the CM group using a SEM image	27
Figure 10: Graph illustrating the mean width of the IAI micro-gap in group 1 and 2	29
Figure 11: Measurement of the depth of the IAI on the left and right sides of the GM group assembly using micro CT scan	31
Figure 12: Measurement of the depth of the IAI on the left and right sides of the CM group assembly using micro CT scan.....	31
Figure 13: Graph illustrating the mean values of the IAI in group 1 and 2	32
Figure 14: Graph illustrating the variations in the means of depths within and across the two groups.....	33
Figure 15: The tilting angle of the implant assembly to view the IAI via SEM	38
Figure 16: Measuring the angle of the IAI at the y-z plane using SEM image	38
Figure 17: The width of the IAI in cross sectional plane in micro CT scan image	40

LIST OF ABBREVIATIONS

IAI:	Implant-abutment interface
GM:	Grand Morse
CM:	Cone Morse
SEM:	Scanning Electron Microscope
CT:	Computed Tomography



CHAPTER 1: INTRODUCTION

The use of dental implants as replacements for edentulous spaces has been reported as a highly successful and predictable procedure for many decades (Nascimento *et al.*, 2008). Nevertheless, several factors can be attributed to their occasional failure, such as the peri-implant tissue infection as a result of implant-abutment interface (IAI) microleakage (Scarano *et al.*, 2005). Contemporary implant systems cannot completely prevent microbial leakage to the internal part of the implant (Nascimento *et al.*, 2008). Hence, prevention of this leakage is a major challenge for the construction of modern two-stage implant systems in order to minimize inflammatory reactions and to maximize bone stability at the implant neck (Harder *et al.*, 2010).

Various studies have been conducted in an attempt to gain a more secure connection between the implant fixture and abutment (Nassar & Abdalla, 2015). The internal connection design has shown better sealing in the implant-abutment interface than the external hexagon. This is attributed to the distinct features offered through different internal connection designs (Peñarrocha-Diago *et al.*, 2013).

Different studies reported less microbial penetration of the internal conical (Morse taper) connection in comparison to other connection designs when using various small microbial molecules or their products (Koutouzis *et al.*, 2011; Jaworski *et al.*, 2012). Therefore, the aim of this *in vitro* laboratory analysis is to investigate the sealing ability of an implant system with a novel connection design at the implant-abutment interface. The hypothesis to be tested is that the novel conical (Morse taper) internal hexagon connection is tight enough to prevent bacterial leakage through the implant-abutment interface.

CHAPTER 2: LITERATURE REVIEW

2.1 Background:

Over the past three decades, the use of dental implants in dentistry has proven to be a successful technique in replacing missing teeth (Coelho *et al.*, 2008). The basic concept of dental implants consists of placing a root analogue, or a fixture, inside the alveolar bone. This is used to support an abutment of single or multiple dental prosthetic replacements (Broggini *et al.*, 2003).

The fixture's top is placed at the alveolar bone level and after a certain period of time it is connected to the abutment, commonly done by means of screw-type connection (Broggini *et al.*, 2003). This system allows for a longer healing period and successful osteointegration (Watchel *et al.*, 2016). However, the disadvantage of this system is the presence of a micro-gap between the abutment and the implant fixture connection, also termed the implant-abutment interface (IAI) (Jansen *et al.*, 1997). However, the implant system can be formed by one piece with the top superior to the bone level (Broggini *et al.*, 2003).

This micro-gap entraps different microbial organisms, leading to peri-implant tissue inflammation, bone loss and implant failure (Ericsson *et al.*, 1995; Broggin *et al.*, 2003; Harder *et al.*, 2010). Furthermore, any mobility between the two implant parts can widen the micro-gap causing further bacterial leakage (Harder *et al.*, 2010). In line with the above, recent studies (Do Nascimento *et al.*, 2012; Canullo *et al.*, 2015) have concluded that the use of the two stage implant systems inevitably results in the formation of a micro-gap and consequential bacterial leakage. There are variations in the bacterial leakage through implant-abutment interfaces according to factors such as marginal fit, mobility and torque (Harder *et al.*, 2010; Steinebrunner *et al.*, 2005), and most importantly the type of connection used between implant fixture and abutment (Goiato *et al.*, 2015; Do Nascimento *et al.*, 2012).

2.2 Types of connection design:

The implant systems have been subdivided into two categories according to the types of connection present between the abutment and the fixture (Goiato *et al.*, 2015). These two types are: (1) the external hexagon connection (Figure 1) and (2) the internal connection (Figure 2).



Figure 1: Example of external connection designs (Muley *et al.*, 2012).



Figure 2: Examples of internal connection designs (Muley *et al.*, 2012).

Table 1: Previous work of *in vitro* clinical studies using an external hexagon connection design.

Authors	Sample number (n)	Inoculum types	Follow up period	Evaluation method	Result	Notes
Nascimento <i>et al.</i> , (2008)	Pre -machined n=10; cast assembly n=10	Fusobacterium nucleatum	14 days	Bacterial culture	Mixed	11.1% of assemblies in each group showed bacterial leakage
Barbosa <i>et al.</i> , (2009)	Branemark n=20	Fusobacterium nucleatum	14 days	DNA check board	Mixed	60% of assemblies showed bacterial leakage
Nascimento <i>et al.</i> , (2009a)	Pre-machined (Group 1) n=10; pre-machined (Group 2) n= 10	Streptococcus mutans	14 days	Bacterial culture	Mixed	15% of Group 1 and 35% of Group 2 of the assemblies showed bacterial leakage
Nascimento <i>et al.</i> , (2009b)	Cast abutment n=9; pre-machined n=9	Streptococcus sobrinus	14 days	DNA check board	Mixed	11% of cast abutment and 31% of pre-machined assemblies showed bacterial leakage
Do Nascimento <i>et al.</i> , (2011)	Branemark external hexagon n=12	Saliva	7 days	DNA check board	Positive	100% of assemblies showed bacterial leakage
Dias <i>et al.</i> , (2012)	Neodent n= 10; Conexão n= 10; SIN n= 10; Dentoflex n= 10; Titanium n= 10	Escherichia coli	14 days	Bacterial culture	Mixed	25% of Dentoflex assemblies showed bacterial leakage

2.2.1 External hexagon connection design:

The external hexagon design is the type of connection that has been made available since the development of implant osteointegration (Brånemark *et al.*, 1977). This design is characterized by the anti-rotation mechanism and reversibility properties (Goiato *et al.*, 2015). For these reasons, it accounts for the majority of implant designs in the market according to a recent survey (Dias *et al.*, 2012).

Most studies conducted using implants with external hexagon connections have shown the presence of bacterial leakage regardless of the technical variable used (Table 1). Several studies that have used a more sensitive method of bacterial detection (e.g. DNA checkerboard hybridization) than the bacterial culture have identified higher bacterial counts with the use of an external hexagon design (Barbosa *et al.*, 2009; Nascimento *et al.*, 2009b; do Nascimento *et al.*, 2011).

Other researchers (Dias *et al.*, 2012) proposed that external hexagon connection micro-gap leakage has been exaggerated and that there is no relation between bacterial leakage and implant abutment interface misfits.

Despite this suggestion, it has been proved that an external hexagon has less efficient configuration, attributed to its short platform (Almeida *et al.*, 2013; Costa *et al.*, 2017). The latter causes instability and increases the micro-gap resulting in more bacterial leakage (Almeida *et al.*, 2013; Costa *et al.*, 2017). Studies indicated that the micro-gap size in an external hexagon connection can reach up to 86.6 μm (De Olivera *et al.*, 2014). Hence, the manufacturing of internal connection designs with better geometry was developed to overcome this shortcoming (Binon, 2000).

Table 2: Comparative *in vitro* clinical studies between the external hexagon and different internal connection designs.

Authors	Sample number (n)	Inoculum types	Follow up period	Load	Results		
					Positive	Negative	Mixed
Do Nascimento <i>et al.</i> , (2012)	External hexagon n=20; Internal hexagon n=20; Morse taper n=20	Saliva	7 days	Group1: loaded; Group2: static	External hexagon; Internal hexagon	-	Morse taper
Costa <i>et al.</i> , (2017)	External hexagon n=12; Morse taper n=12	Escherichia coli	14 days	Static	External hexagon	Morse taper	-
Jaworski <i>et al.</i> , (2012)	External hexagon n=12; Morse taper n=12	Escherichia coli	28 days	Static	External hexagon	-	Morse taper

UNIVERSITY of the
WESTERN CAPE

2.2.2 Internal connection designs:

Several internal connection designs are currently used in the market. These designs are (1) conical internal design (Morse taper), (2) internal hexagon and (3) internal octagon (Goiato *et al.*, 2015), with several variations of different types (Shafie & Hamid, 2014).

The internal connection design has shown better sealing in the implant abutment interface than the external hexagon (Peñarrocha-Diago *et al.*, 2013). This has been attributed to the more apical position of the implant-abutment interface away from the alveolar bone crest, the platform switch concept and bone protection by the internal micro-threads geometry (Peñarrocha-Diago *et al.*, 2013).

The conical internal design connections have frictional fit characteristics which depend on frictional resistance in wider implant abutment contact areas. This special feature aims for better sealing and stability (Coppedê *et al.*, 2009). On the other hand, internal hexagons have less contact although they provide more surface area of micro-threads (Coppedê *et al.*, 2009). The incorporation of an internal hexagon or octagon into the conical connection as modification of the original designs provided resistance against lateral and rotational forces, as well as ease of reversibility (Mueley *et al.*, 2012, Ding, 2003).

Studies reported that the micro-gap size in a conical internal connection design is an average of $6.61 \pm 3.17 \mu\text{m}$ (Ranieri *et al.*, 2015). Furthermore, it can reach up to $53.9 \mu\text{m}$ in an internal hexagon design (De Olivera *et al.*, 2014), while the internal octagon design ranges from 7 to $10 \mu\text{m}$ depending on the abutment type used (Rismanchian, 2012).

A comparative *in vitro* study was conducted to evaluate the bacterial leakage among different types of connections. The conical internal design (Morse taper) showed the lowest leakage when compared to an external hexagon in loaded and static conditions (do Nascimento *et al.*, 2012), and similar results have been obtained by other researchers irrespective of the methods used (Table 2). Moreover, the cross-sectional *in vivo* study by Canullo *et al.* (2015), comparing both types of connection in terms of sealing capacity, has shown superior results using internal connection designs.

Garrana *et al.* (2016) attempted to detect and measure the amount of bacterial endotoxin leakage through testing external hexagon connections against different types of internal connection designs. This study reported no leakage in both Morse taper and conical designs with internal octagon connection designs. Moreover, the internal octagon connection showed better results than the external hexagon design.

Table 3: *In vitro* clinical studies using different internal connection designs.

Authors	Sample number (n)	Direction	Inoculum types	Follow up period	Loading	Result	Notes
Dibart <i>et al.</i> , (2005)	Internal Connection n=25	External to internal surface (E/I); Internal to external surface (I/E)	Mixture of bacteria	E/I: 24 hours; I/E: 72 hours	Static	positive	100% of the assemblies showed negative bacterial leakage
Coelho <i>et al.</i> , (2008)	Intra Lock n=5; Strauman n=5; Trilobe n=5	Internal to external surface (I/E)	Toluidine blue	7 days	Static	Mixed	22% of Intra-Lock, 55% of IC and 100% of Trilobe of the assemblies showed positive bacterial leakage
Teixeira <i>et al.</i> , (2011)	Internal hexagon n=10; Morse taper n=10	External to internal surface (E/I), Internal to external surface (I/E)	Staph. aureus	I/E: 7 days; E/I: 14 days	Static	Mixed	70% of both Groups of the assemblies showed positive bacterial leakage
Koutouzis <i>et al.</i> , (2011)	Morse taper n=14; conical grooved n=14	External to internal surface	E. coli	500,000 cycle (N15)	Loaded	Mixed	7% of Morse taper and 85% conical grooved showed positive bacterial leakage
Aloise <i>et al.</i> , (2010)	Taped-in Morse taper n=10; screwed-in Morse taper n=10	Internal to external surface (I/E)	Strep. sanguinis	14 days	Static	Mixed	20% of both Groups showed positive bacterial leakage
Harder <i>et al.</i> , (2010)	Astra Tech n=8; Ankylose Plus n=8	Internal to external surface (I/E)	Endotoxin	7 days	Static	Mixed	86% of Astra Tech and 100% Ankylose Plus showed positive bacterial leakage

A comparative study by Peñarrocha-Diago *et al.* (2013) using radiographic evidence showed more bone loss as a result of bacterial leakage in the external hexagon than the internal connection design. There are several other studies that compared variable internal connection designs using different methodologies (Table 3). Some of those studies have shown that bacterial leakage can occur through all directions, either from the external surface of the implant to the interior, *vice versa*, or even in both directions. Moreover, the type and volume of the inoculum were other variables used in some of the studies. These researchers used saliva, stains and different types of bacteria ranging from facultative to obligate anaerobic bacteria, or even as small as bacterial endotoxin, to produce more accurate results (Table 3). Da Silva-Neto (2012) justified the use of bacterial endotoxins as they are the main cause of peri-implant bone loss. The use of bacteria in most of the studies is attributed to their small sizes, easy passage through the micro-gap and to mimic the peri-implant area (da Silva-Neto, 2012; Table 3).

Streptococcus sanguinis is one of the bacterial strains used in bacterial leakage studies (Aloise *et al.*, (2010). The use of this gram-positive, facultative, anaerobic bacterium, to test the bacterial leakage was justified by its small size (0.5-1 μ m) and frequent presence in the peri-implant environment (Da Silva-Neto *et al.*, 2012). In addition to being one of the major primary colonizers of the oral biofilm, it has the ability to adhere to the implant titanium surface and facilitate the adherence of the secondary microbial colonizers (Ranieri *et al.*, 2015).

Dibert *et al.* (2005) conducted a bidirectional *in vitro* study to test the sealing capacity of implants with a locking taper internal connection design against bacteria. Their results showed that none of the samples had signs of bacterial leakage in both directions proving a hermetic sealing of the locking taper connection against different types of bacteria (Dibert *et al.*, 2005). A few years later, Coelho *et al.* (2008) rejected the null hypothesis based on the results they obtained using three types of internal connection designs (e.g. Morse taper, tri-lobe internal connection and Intra-lock's modified hexagon). They found positive results in all types with varying degrees; i.e 22% in Intra-Lock, 55% in Morse taper and 100% in tri-lobe internal connections (Coelho *et al.*, 2008).

Teixeira *et al.* (2011) investigated bacterial leakage in both directions between internal hexagon and Morse taper connections and found positive results in both groups with no statistical difference. Koutouzis and his co-workers (2011) submitted two different internal connection systems (Morse taper and four-groove conical internal connection) to bacterial culture under loading of a wear simulator. They detected that 7% of Morse taper and 85% of

conical grooved designs showed bacterial leakage suggesting that difference in connection designs can give variable results under loading (Koutouzis *et al.*, 2011). Alois *et al.* (2009) investigated whether different types of the same design would show different bacterial leakage risks using two commercially available Morse taper systems. They later detected the presence of bacterial leakage in all types with no statistical differences. In another study, Harder *et al.* (2010) used smaller molecules than whole bacteria, which are the endotoxins, to investigate micro-leakage through smaller micro-gaps. They conducted their study using two commercial different internal conical connection systems and both systems showed bacterial leakage at variable time intervals.

As previously mentioned, the bacterial leakage through the implant-abutment interface is influenced by the connection stability which in turn is affected by its geometry (Harder *et al.*, 2010; Binon, 2000). Studies have reported high mechanical stability of implants with Morse taper type of connections (Sasda & Cochran, 2017). They reported that the “cone in a cone” design of this type of connection would provide a secure and strong cold welding between the implant and the abutment (Binon, 2000). Moreover, Ranieri *et al.* (2015) investigated the sealing ability of 4 different Morse taper implants against bacteria and concluded that the taper angle and the amount of torque used on the IAI play a determining role in the stability and the sealing ability of the connection. In this context, Morse taper connections have different taper angles available on the market such as 1.5, 8 or 11.5 degrees between the two parts (Mueley *et al.*, 2012). Furthermore, Sasada and Cochran (2017) suggested that the longer the contact between the implant fixture and the abutment, the more stable the connection.

The microbial leakage is possibly related to the size of the IAI and marginal misfit (Nassar and Abdullah, 2015). Several studies attempted to measure the size of the micro-gap using different techniques (Ranieri *et al.*, 2015; de Faria *et al.*, 2013). The Scanning Electron Microscope (SEM) scans the topography and configuration of a sample by an electron beam to produce a high-resolution magnified image. It is one of the major techniques used for detecting and measuring the IAI (De Faria *et al.*, 2013). Another reliable method for the IAI evaluation is the use of the micro CT scanning (micro CT). The micro CT is a three dimensional method that provides highly magnified detailed images characterized by high resolution and contrast (Yip *et al.*, 2004).

2.3 A Novel Implant Connection:

Currently, new connections have been developed such as the novel Grand Morse (GM) connection design offered through Neodent® implant system, Straumann AG, Basil, Switzerland.

The developers of this novel implant connection claim that it has a unique design consisting of several distinctive features: a 16° deep conical and hexagon internal connection associated with a wide platform switch (Neodent® Implant Systems Inc., 2018). The presence of a 16° deep frictional fit conical connection offers a large contact area between the implant and the abutment for a wide load distribution and ultimate sealing (Figure 3: A-3,4). In addition to the presence of six internal indexing features allowing for precise placement of the abutment, it has an anti-rotation facility and is easy to use (Neodent® Implant Systems Inc., 2018) (Figure 3: A-1). The GM connection design also provides a wide platform switch which is an abutment with a narrower diameter than the implant to reduce crestal bone loss (Cumbo *et al.*, 2013) (Figure 3: A-2). This platform allows for a persistent and compact soft tissue seal around the implant-abutment connection, efficient frictional fit, supreme abutment stability and no micro-movements between implant and abutment (Neodent® Implant Systems Inc., 2018). These features offer a secure and durable design based on proven concepts (Neodent® Implant Systems Inc., 2018).

In addition, the developers of this novel connection claim that it has shown promising results with regard to high primary stability, reliable osseointegration, successful prosthetic restoration and aesthetic superiority (Neodent® Implant Systems Inc., 2018).

However, the sealing ability of the novel connection design to bacterial leakage has not yet been established (Figure 3-B; Table 4).

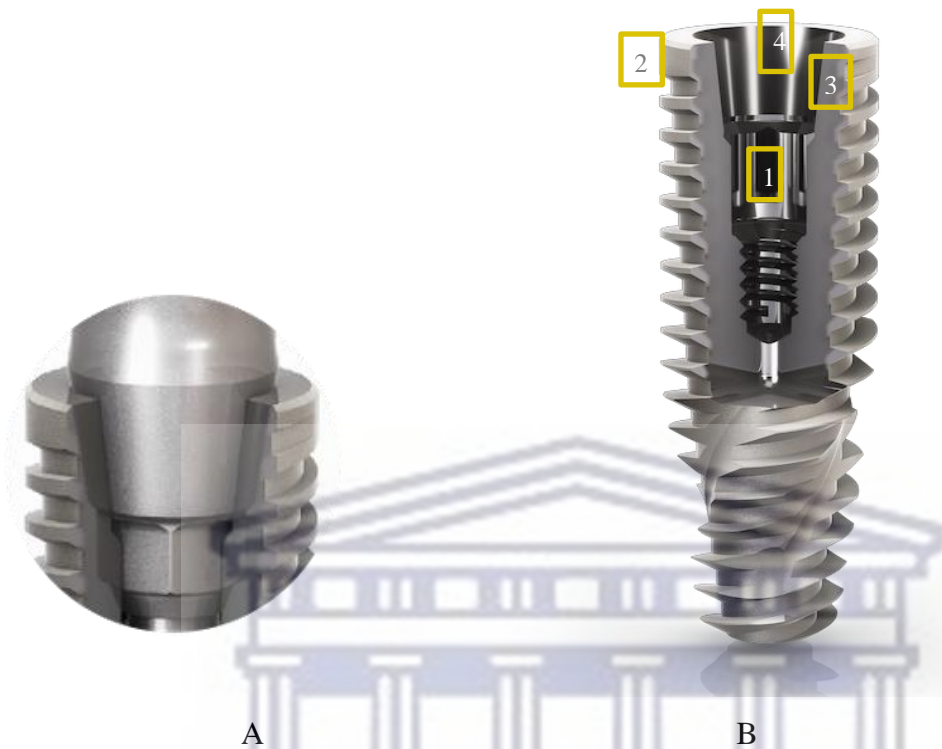


Figure 3: A- The novel GM implant connection. B- Dimensions of the GM connection in Helix GM implants:(1) Internal hexagon, (2) Platform switching, (3) Deep implant-abutment interface, (4) 16°Morse taper connection (Neodent® Implant Systems Inc., 2018).

Table 4: Characteristics of GM connection design (Neodent® Implant Systems Inc., 2018).
(Figure 3).

Connection Feature	Dimension
Connection Design	Conical internal hexagon connection
Internal Connection Diameter	3 mm
Connection Depth	3.70 mm
Total Depth of the Connection (including the screw)	6.60 mm
Angle of the Conical connection	16°
Special features	Wide platform switching with deep IAI.

4.3.2 The Rationale of the Study:

The rationale of this study was based on the ongoing search for an implant design that could offer hermetic sealing at the implant-abutment interface. An implant with a novel conical internal hexagon connection design claims to combine features in one implant system that offers hermetic sealing at the implant-abutment interface (Neodent® Implant Systems Inc., 2018).

Hence, the study of bacterial leakage of a novel implant-abutment interface at the Faculty of Dentistry, University of the Western Cape, Tygerberg campus, is conducted in view of this achievement.

The purpose of this study was to evaluate the bacterial leakage along the implant-abutment interface of an implant with a novel connection design *in vitro*. Therefore, the hypothesis to be tested is that the novel GM connection is tight enough to prevent bacterial leakage through the implant-abutment interface.

CHAPTER 3: AIMS AND OBJECTIVES

3.1 Aim:

The aim of this study was to test the sealing ability against bacterial leakage in the implant-abutment interface provided by an implant with a novel deep internal conical (GM) connection design.

3.2 Objectives:

- a. To determine bacterial growth within an implant with a GM connection design by using bacterial analysis.
- b. To determine bacterial growth within an implant with a CM connection design using bacterial analysis.
- c. To measure the size of the implant-abutment interface micro-gap of an implant with a GM connection design by using scanning electron microscopy (SEM).
- d. To measure the size of the implant-abutment interface micro-gap of an implant with a CM connection design by using scanning electron microscopy (SEM).
- e. To measure the length of the implant-abutment interface of an implant with a GM connection design by using micro Computer Tomography (CT) scanning.
- f. To measure the length of the implant-abutment interface of an implant with a CM connection design by using micro Computer Tomography (CT) scanning.
- g. To compare the bacterial sealing capacity between an implant with a GM connection design and an implant with a CM connection by using bacterial analysis, scanning electron microscopy (SEM) and micro Computer Tomography (CT) scanning.

CHAPTER 4: MATERIALS AND METHODS

4.1 Study design:

The present study conducted an *in vitro* laboratory analysis to investigate the sealing ability of an implant system with a novel connection design at the implant-abutment interface. The use of an *in vitro* as opposed to an *in vivo* study, resulted in more accurate results due to the fact that bacterial contamination of the interior is unpreventable in the latter (Persson *et al.*, 1996) while in the former, the implant is assumed to be sterile from the start (Canullo *et al.*, 2015).

In vitro analysis was conducted at the Department of Oral Medicine and Periodontology, Oral and Dental Research Laboratory, Tygerberg Campus, University of the Western Cape.

4.2 Sample size:

A total of 20 dental implants (Biocompatible titanium alloy 4.3 x10mm) (Neodent® Implant Systems Inc., Straumann AG, Basel, Switzerland) and corresponding abutments were exposed to the microbial challenge (Table 5). Group 1 was composed of ten implants from the **Helix GM** implant system with a novel GM connection design (Figure 4: A). Group 2 contained an equal number of samples from **Drive CM** Implant, an implant system with an internal conical (Morse taper) connection design (Figure 4: B). The Drive CM implant was chosen for comparison with Helix GM due to the presence of similar features such as the Morse taper connection called Cone Morse (CM). The Neodent company claimed that the CM connection was effective in preventing microbial leakage according to a recent report published on their website (Neodent, 2018). The number of samples was chosen from an average of 18 studies mentioned in a systematic review by da Silva-Neto (2012) where the number of samples used varied between 3 and 30.

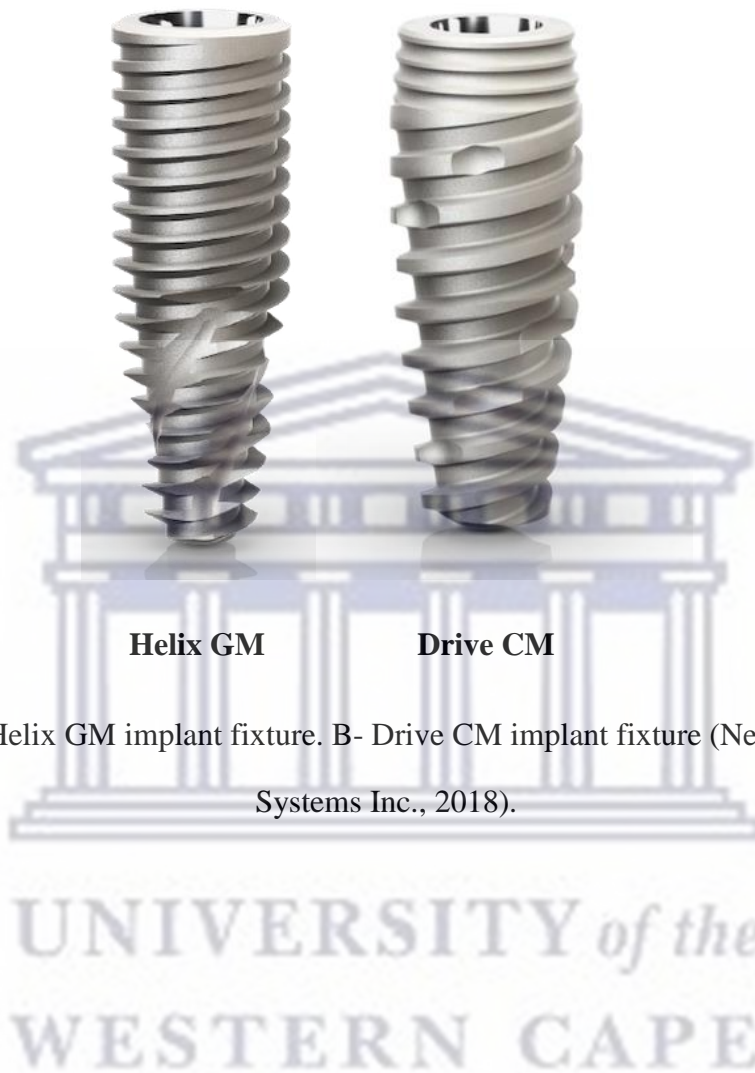


Figure 4: A- Helix GM implant fixture. B- Drive CM implant fixture (Neodent® Implant Systems Inc., 2018).

Table 5: Characteristics of the implants included in the current study.

Study by	Helix GM	Drive CM
Implant size	4.3 x10mm	4.3 x10mm
Connection design	Grand Morse connection (GM)	Cone Morse connection (CM)
Surface	Sand blasting, acid etching	Sand blasting, acid etching
Material	Titanium alloy	Titanium alloy
Internal Connection Diameter	3 mm	2.5 mm
Depth of the Connection	3.70 mm	4.1 mm
Angle of the Conical connection	16°	11.5°

4.3 Methodology:

The following methodological steps were adopted from previous studies (Nassar & Abdullah, 2015; Ranieri *et al.*, 2015) in this laboratory investigation.

4.3.1 Bacterial Culture Preparation:

Streptococcus sanguinis (ATCC10556) was the microorganism used to test the bacterial sealing capacity of the novel implant abutment connection for the current study. The justification for choosing this microorganism during the analysis was because it is one of the major primary colonizers of the oral biofilm and has the ability to adhere to the implant titanium surface and facilitate the adherence of the secondary microbial colonizers (Ranieri *et al.*, 2015).

A brain–heart infusion (BHI) broth was used for the growth of *S. sanguinis*. It is composed of brain and heart tissue infusion forming a culture that provides the necessary nutrients for microbial growth (Ronald *et al.*, 1980).

100 ml of a brain–heart infusion (BHI) broth was prepared according to the manufacturer’s instructions. To ensure optimum sterile conditions, the broth’s bottle was sterilised in an autoclave at 121°C for 15 minutes.

S. sanguinis bacteria were donated by the dental research laboratory and were grown in BHI and cultured in labelled agar plates. These plates were then placed in an incubator for 18 to 24 hours at 37°C and 5% CO₂ incubation measures.

The bacterial inoculum was extracted from the 18-hours-old culture and diluted in phosphate buffered solution (PBS). The suspensions were adjusted to 0.5 of the McFarland standard turbidity, 10⁸ colony forming units/mL (Ranieri *et al.*, 2015).

4.3.2 Bacterial Challenge:

Twenty-four hours prior to bacterial inoculation, all the abutments were sent for gas sterilisation to exclude contamination on the abutment surfaces. Under sterile conditions, all implant fixtures were removed from their packaging using sterile pliers (Ranieri *et al.*, 2015).

This was followed by using a micro-pipette to inject 0.05 ml of sterile BHI inside each implant well to mimic the oral fluid leakage usually occurring during surgery and to provide nutrition for bacterial growth if they crossed the IAI seal (Ranieri *et al.*, 2015). Thereafter, each implant was carefully connected to the corresponding abutment according to the manufacturer’s instructions. This was done by using a sterile clamp to hold the implant assembly allowing a firm screwing action. Group 1 fixtures were connected to their standard abutments using a screw with a torque value of 25 Ncm according to the manufacturer’s protocol; group 2 fixtures were connected to their corresponding abutments with a torque

value of 15 Ncm according to manufacturer's recommendations (Figure 1; Refer to appendix A). Thereafter, the implant assemblies were directly submerged in glass tubes containing 4 ml of sterile BHI to a level above the IAI but below the screw opening (Jansen *et al.*, 1997) (Figure 2; Refer to appendix A). This level was determined to ensure that if leakage occurred, it would result from leakage through the IAI and not from the screw opening. These glass tubes were all sent for autoclave sterilisation at 121°C for 15 minutes to ensure complete sterility before adding bacteria.

0.01ml (10 µl) of bacterial culture suspension of 10 µl was added to the sterile BHI in which the implants were submerged and incubated for 48 hours at 37°C 5% CO₂ as done in previous studies (Nassar & Abdullah, 2015).

After 48 hours of incubation, the assemblies were removed from the test tubes using sterile pliers, sprayed with 70% alcohol and placed vertically in a stand for 10 minutes until the alcohol had evaporated (Figure 3: A-B; Refer to appendix A). The assemblies were disconnected aseptically using a sterile torque wrench. For each implant, the implant's inner surface was sampled by sterile paper points for bacterial contamination (Figure 4; Refer to appendix A). The paper points were immersed in labelled test tubes containing 1000 µl of sterile BHI, for 20 minutes (Figure 5; Refer to appendix A). A tube containing the same BHI used to detect bacteria inside the implant was immersed with a sterile paper point as negative control to exclude BHI contamination. All the BHI tubes containing paper points were cultured on labelled agar plates (TSA with LTHTh-ICR Contact Plates GRN: ST16/0128). These plates were incubated at 37 °C for 24 hours (Nassar and Abdullah, 2015).

After 24 hours, the agar plates were collected and examined for bacterial growth whereas plates with growth underwent colony counting. The widely accepted range of 30-300 CFU per plate was used in which <30 was considered insignificant, while >300 were considered too numerous to count (Sutton, 2011). Thereafter, Gram's staining was done on selected colonies to confirm that they were *Streptococcus sanguinis* (Nassar and Abdullah, 2015).

4.3.3 Scanning Electron Microscopy:

The Scanning electron microscopy (SEM) analysis was conducted at the Electron Microscope Unit, Physics Department, University of the Western Cape.

Scanning electron microscopy (SEM) was used to measure the size of the implant-abutment interface micro-gap of the implant assemblies.

To generate a SEM image, a Windows programmed computer with software (Zeiss SmartSEM, Carl Zeiss, Oberkochen, Germany) was used to control the process with a handle to control the angles and position of the samples.

A random selection of two implant assemblies from the positive samples that showed growth in each group was done to perform SEM analysis. The two assemblies were chosen randomly to exclude manufacturers' errors or defects that might occur in samples.

For the preparation of the samples to undergo the SEM analysis, the assembly components were sterilized by using an ultrasonic cleaner and then reconnected. The sample size was increased by performing multiple readings on each implant assembly. The IAI micro-gap was measured in 12 random points at the interface external entrance using a magnification power of $\times 1.39k$. The micro-gap was measured in micrometers (μm) by drawing a line from the abutment to the implant surfaces on the produced image (Figure 6 & 7; Refer to appendix A).

4.3.4 Micro Computer Tomography (CT) scanning:

The micro CT scanning analysis was conducted at the CT scan laboratory, Central Analytical Facility, University of Stellenbosch. It was used to measure the length (depth) of the IAI at different equidistant points of a single implant from each Group.

A Viewer graphics software (myVGL 3.2, Helderberg, Germany) was used to view and analyse images created by VGSTUDIO MAX and VGSTUDIO interactively and in three dimensional view.

In each group, one of the samples that had under gone SEM analysis was chosen to perform micro CT scanning. The sample size was increased by performing multiple readings on each implant assembly. The two assemblies were chosen randomly to exclude manufacturers' errors or defects that might occur in the samples.

For the preparation of the samples, the assembly components were sterilized by using an ultrasonic cleaner, reconnected and then scanned for an hour each to produce the requested cross-sectional images.

For the GM connection group, the first step was to measure the depth of IAI at the y-z axis around the connection diameter. This was achieved by drawing a line along the contact between the implant and the abutment on the left (L) and the right (R) sides of the assembly at equidistant points: $500\mu m$, $250\mu m$, $0.00\mu m$, $-250\mu m$ and $-500\mu m$ in the scene coordinate system (Figure 8: A; Refer to appendix A). This resulted in the production of 10 measurements on the y-z plane. The same was performed on the x-z axis which resulted in the production of 10 additional measurements (Figure 8: B; Refer to appendix A).

For the CM connection group, measurement of the depth of IAI at the y-z axis around the connection diameter was performed. This was achieved by drawing a line along the contact between the implant and the abutment on the left (L) and the right (R) sides of the assembly at equidistant points: 500 μ m, 250 μ m, 0.00 μ m, -250 μ m and -500 μ m in the scene coordinate system (Figure 9: A; Refer to appendix A). This resulted in the production of 10 measurements on the y-z plane. The same was performed on the x-z axis which resulted in the production of 10 additional measurements (Figure 9: B; Refer to appendix A).

4.4 Data Collection and Analysis:

Each sample was coded to permit blind analysis. The data were collected by the same investigator, recorded in Microsoft Excel[®] spreadsheets (Microsoft Corporation, USA) and processed using various statistical analysis techniques.



CHAPTER 5: RESULTS

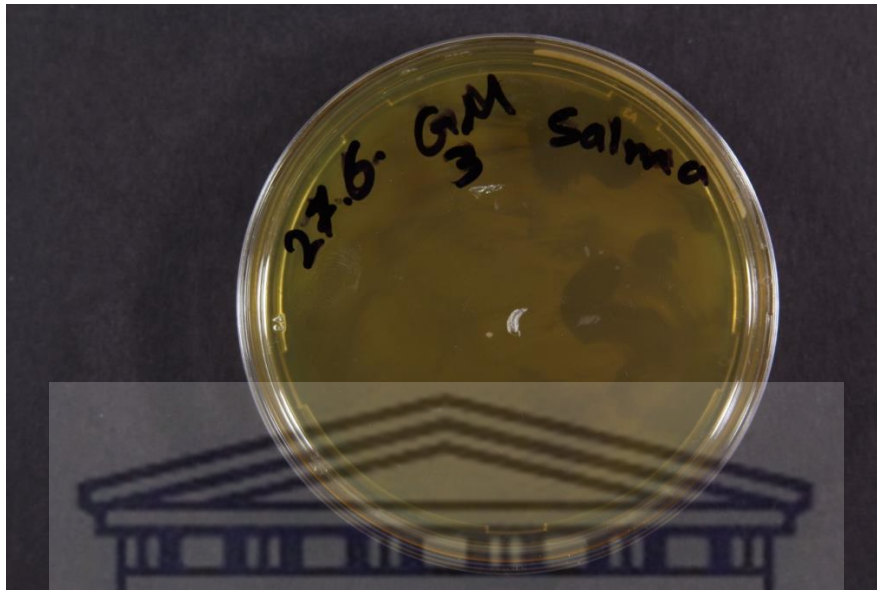
In the present study, laboratory analysis to investigate the sealing ability of an implant system with a novel connection design at the implant-abutment interface was conducted. This was achieved by bacterial analysis to investigate bacterial leakage through the IAI, measuring and comparing the IAI width, length, and angle in groups 1 & 2.

Data were reflected through the use of descriptive statistics and the Chi-square. The Chi-square test was used for comparison of presence or absence of bacterial leakage in both groups.

The mean value and standard deviation of each implant assembly micro-gap in both groups was calculated. Thereafter, the data obtained from both groups were compared by using an independent t-test. For statistical significance, a value of 5% ($P \leq 0.05$) was considered acceptable (Ranieri *et al.*, 2015). IBM^{®1} SPSS^{®2} Statistics Version 20 for Windows (SPSS[®], Inc. Chicago, IL, USA) and Microsoft Excel 2010 (Microsoft Corporation, USA) were used for all the statistical analysis.

5.1 Bacterial Challenge:

In the bacterial leakage analysis, Table 1 (Refer to appendix B) showed bacterial growth in 2 out of 10 assemblies (in number 7 and 10) in the GM connection group (Figure 5), while in Table 2 (Refer to appendix B), the CM connection group showed bacterial growth in 5 out of 10 assemblies (in number 4, 5, 6, 7 and 10) (Figure 6). For each plate that exhibited growth, colony counting was performed. No bacterial colony growth was detected in the negative controls in both groups.

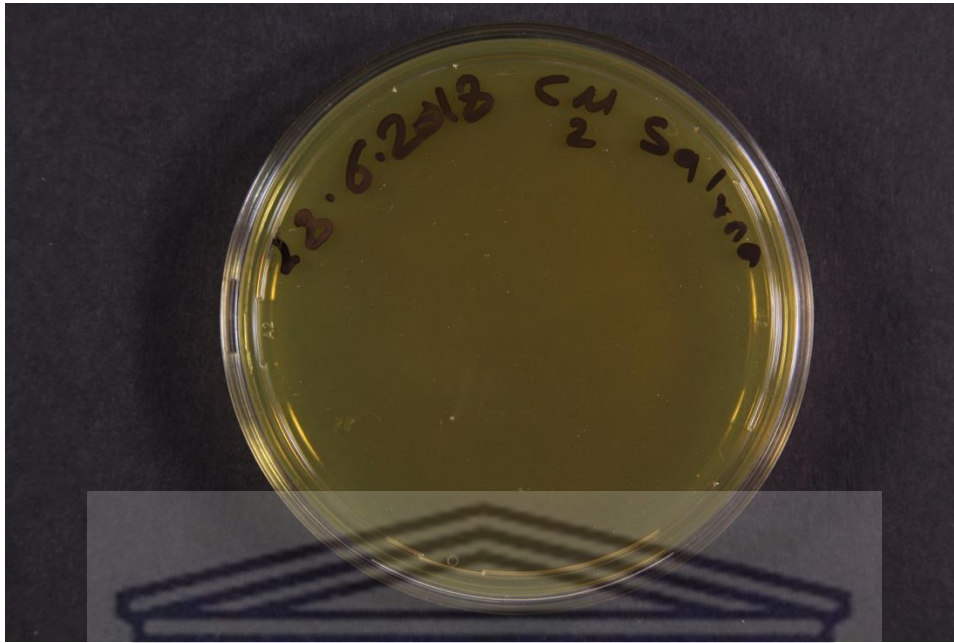


A

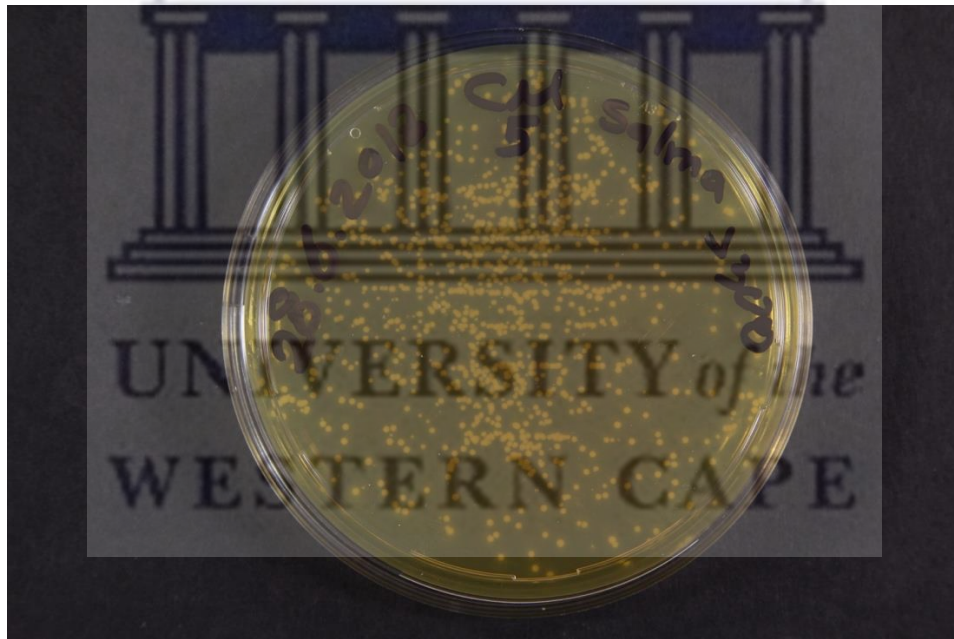


B

Figure 5: Samples of the GM group labelled agar plates. A-No bacterial growth in agar plate number 3. B- Bacterial growth in agar plate number 7.



A



B

Figure 6: Samples of the CM group labelled agar plates. A- No bacterial growth in agar plate number 2. B- Bacterial growth in agar plate number 5.

Table 6: The **Chi-Square Tests** used for comparison of presence or absence of bacterial leakage in both Groups.

Value	df	Asymptotic Significance (2-sided)	Exact Sig. (2-sided)	Exact Sig. (1-sided)
1,978 ^a	1	0,160	0,350	0,175
0,879	1	0,348		
2,027	1	0,155	0,350	0,175
			0,350	0,175
20				

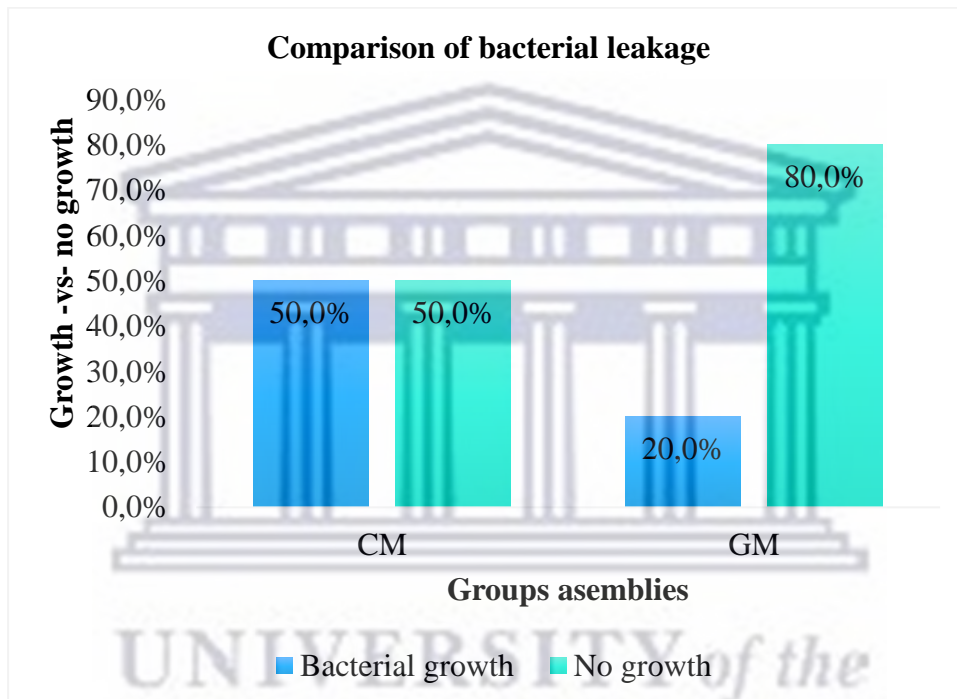


Figure 7: Graph illustrating the bacterial leakage in the GM and CM groups.

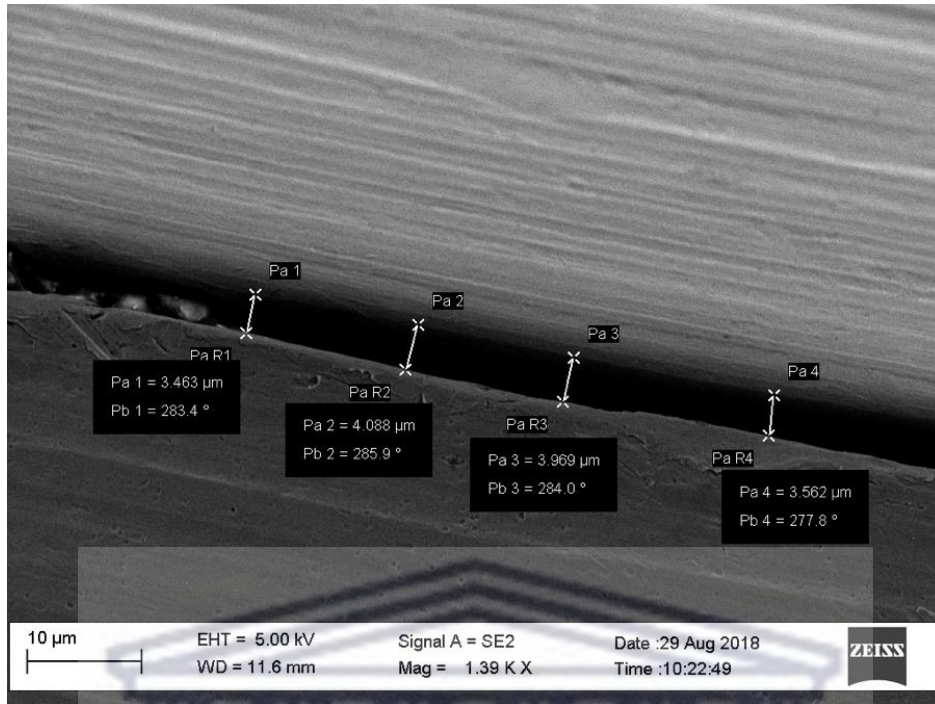
The Chi-square test was performed to determine the presence or absence of bacterial leakage in the GM and CM connections, and whether there were differences between the groups (Table 6).

The results showed that the bacterial leakage was higher in the CM group = 50% compared to the GM group = 20% (Figure 7). However, there were no significant statistical differences between the groups regarding the bacterial leakage, $p = 0.175$ (Table 6).

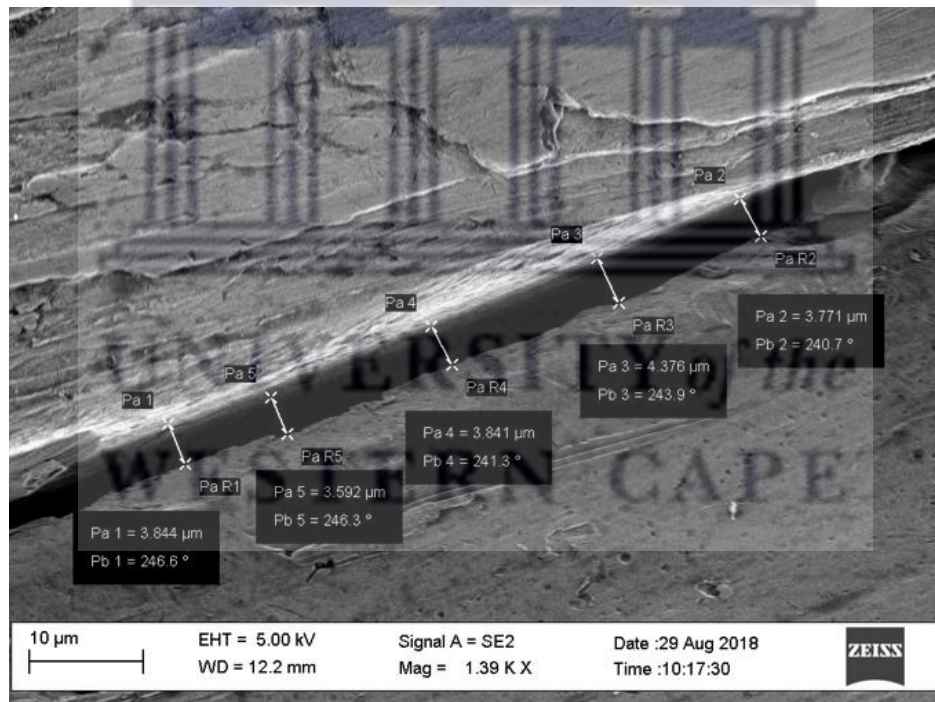
5.2 Scanning Electron Microscopy:

For the SEM analysis, the IAI was measured at 12 random points at the interface of the external entrance using a magnification power of x1.39k. The measurements were reflected in micro-meters (μm) by drawing a line from the abutment to the implant surfaces at the IAI on the produced image (Figure 8). Table 3 (Refer to appendix B) shows the twelve readings of the IAI width for both samples in the GM group, while Table 4 (Refer to appendix B) reports the twelve readings in the CM group samples (Figure 9).



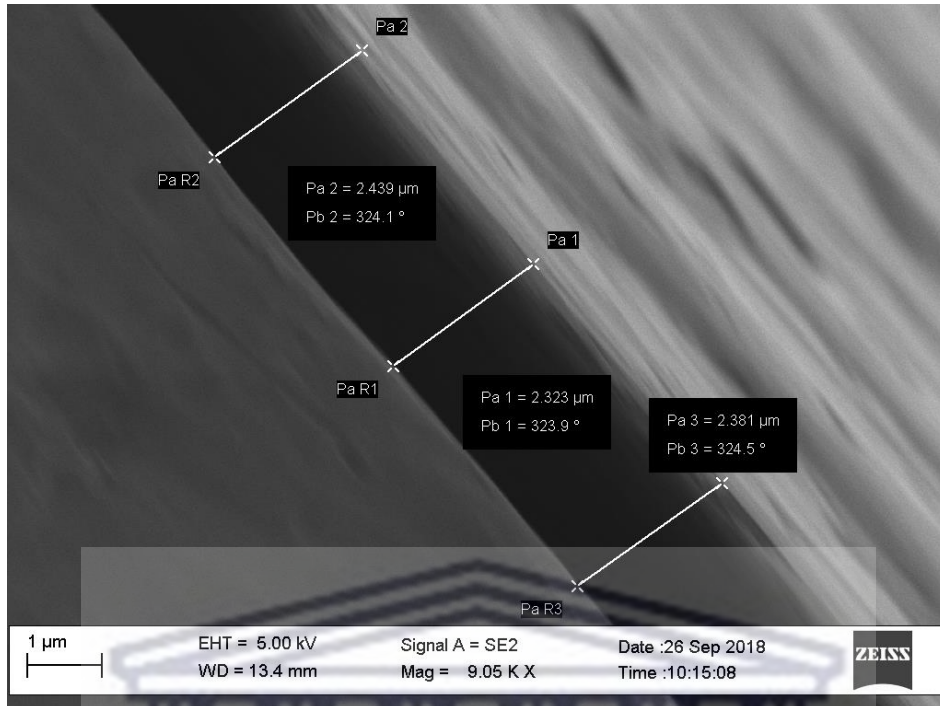


A

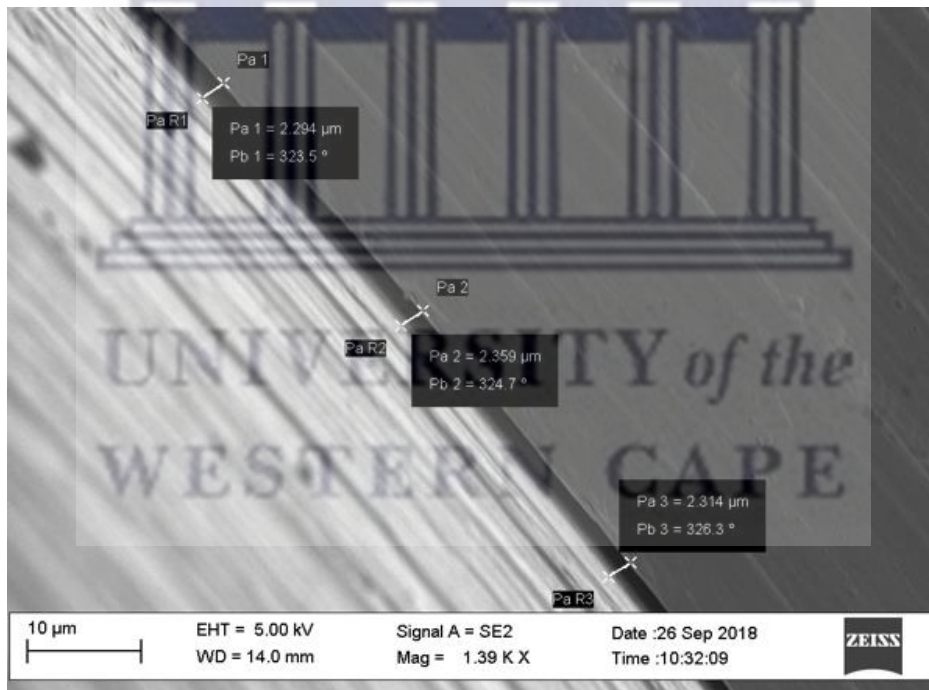


B

Figure 8: Measurement of the interface of the external entrance, in micrometre, at random points in implant assemblies from the GM group using a SEM image. A- Sample no.1, B- Sample no. 2 (magnification of x1.39k).



A



B

Figure 9: Measurement of the interface of the external entrance in micrometre at random points in implant assemblies from the CM group using a SEM image. A- Sample no.1, B- Sample no. 2 (magnification of x1.39k).

Table 7: An independent t-test used for comparison of the mean width and standard deviations in both groups.

Levene's Test for Equality of Variances		t-test for Equality of Means						
F	Sig.	t	df	Sig. (2-tailed)	Mean Difference	Std. Error Difference	95% Confidence Interval of the Difference	
							Lower	Upper
11,099	0,002	16,499	46	0,000	1,754958	0,106366	1,540856	1,969061
		16,499	36,368	0,000	1,754958	0,106366	1,539315	1,970602
	N	Mean	Std. Deviation					
GM	24	4,05	0,45					
CM	24	2,29	0,26					

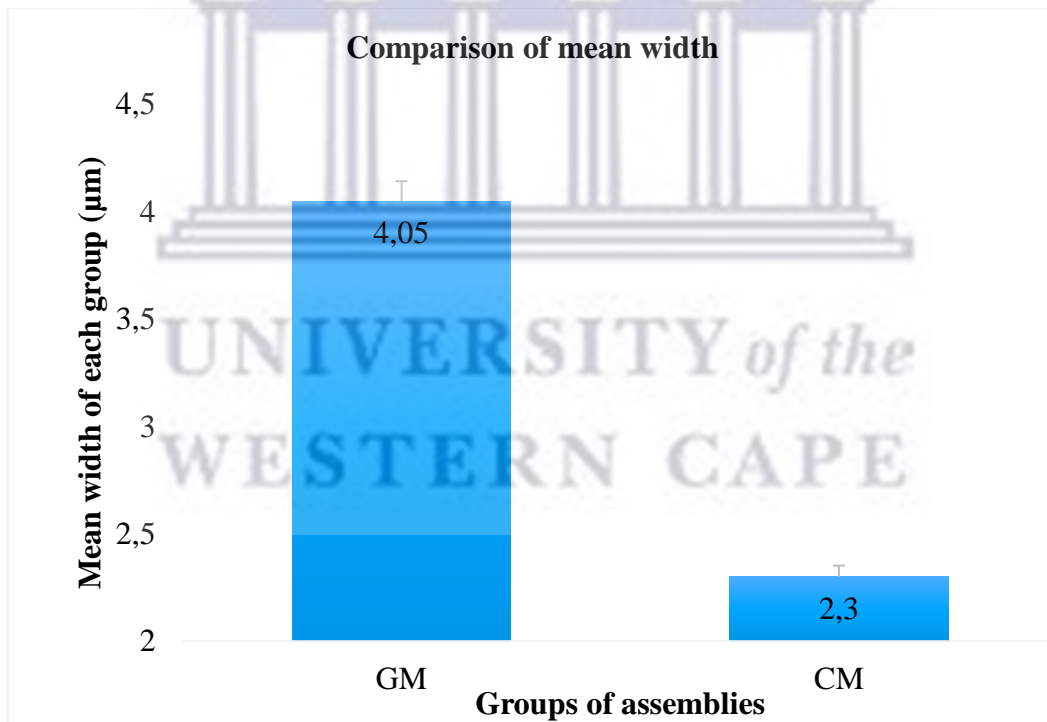


Figure 10: Graph illustrating the mean width of the IAI micro-gap in group 1 and 2.

Statistical data were mean values and standard deviations that were subjected to an independent t-test for comparison between the IAI micro-gap width in the GM and CM groups. The measurement was higher in the GM group, (4.05 ± 0.45) μm , while for the CM

group it was $(2.29 \pm 0.26) \mu\text{m}$ (Table 7). Moreover, there was a statistically significant difference between the groups ($p = 0.00$). These results are shown in Figure 10.

5.3 Micro Computer Tomography (CT) scanning:

For investigating the depth of the IAI, the micro CT scanning analysis produced 10 measurements on the y-z axis and an additional 10 measurements on the x-z axis (Figure 11 and 12). Table 5 (Refer to appendix B) showed the measurements on both axes for the two samples from the GM group, while Table 6 (Refer to appendix B) showed the data obtained from both samples in the CM group.



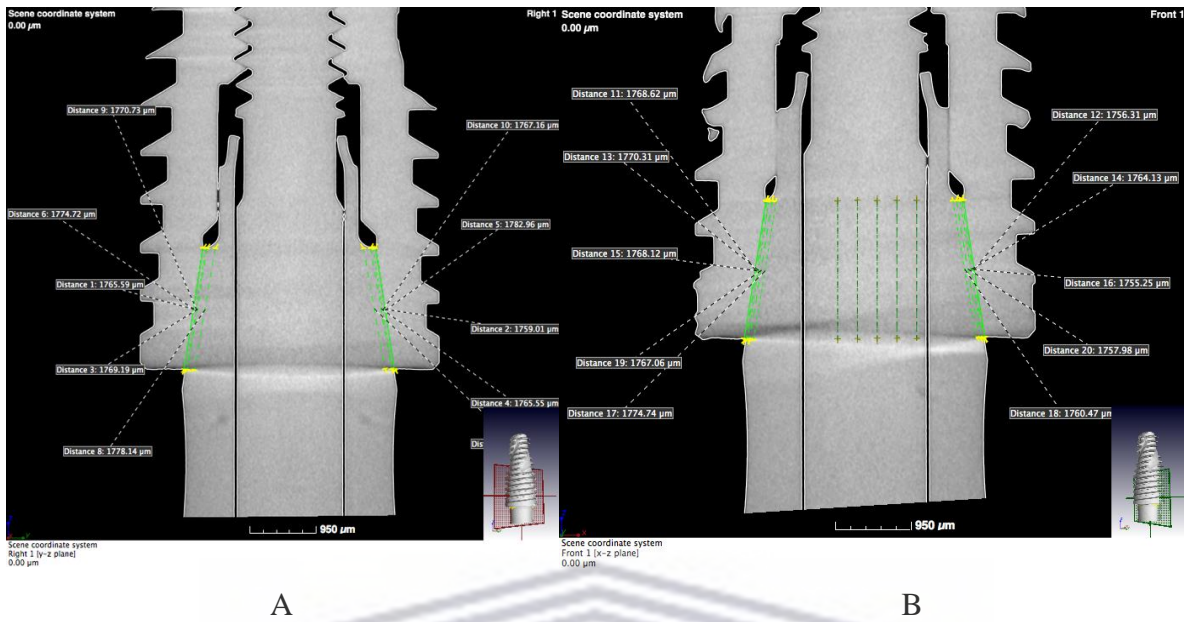


Figure 11: Measurement of the depth of the IAI on the left and right sides of the GM group assembly using micro CT scan. A- At 0.00 µm point on the y-z plane. B- At 0.00 µm point on the x-z plane (magnification of x950 µm).

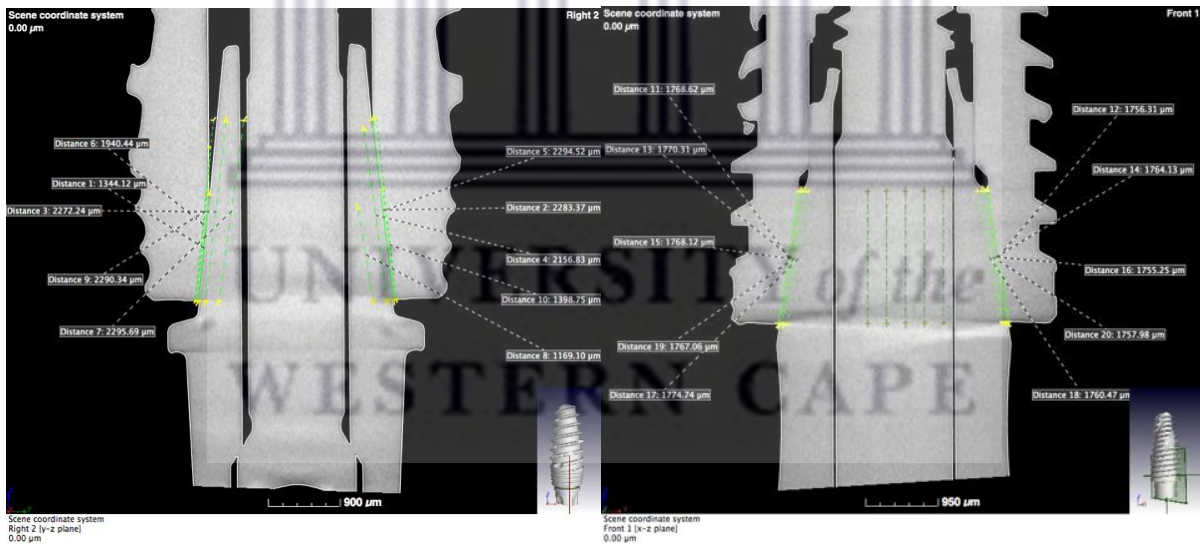


Figure 12: Measurement of the depth of the IAI on the left and right sides of the CM group assembly using micro CT scan. A- At 0.00 µm point on the y-z plane. B- At 0.00 µm point on the x-z plane on the x-z plane (magnification of x950 µm).

Table 8: An independent t-test used for comparison of the mean values and standard deviations in both groups.

Levene's Test for Equality of Variances		t-test for Equality of Means						
F	Sig.	t	df	Sig. (2-tailed)	Mean Difference	Std. Error Difference	95% Confidence Interval of the Difference	
							Lower	Upper
48,085	0,000	-2,107	38	0,042	-198,632	94,271	-389,474	-7,790
		-2,107	19,011	0,049	-198,632	94,271	-395,936	-1,328

	Mean	Std. Deviation	Std. Error Mean
GM	1766,89	7,301	1,632
CM	1965,52	421,531	94,257

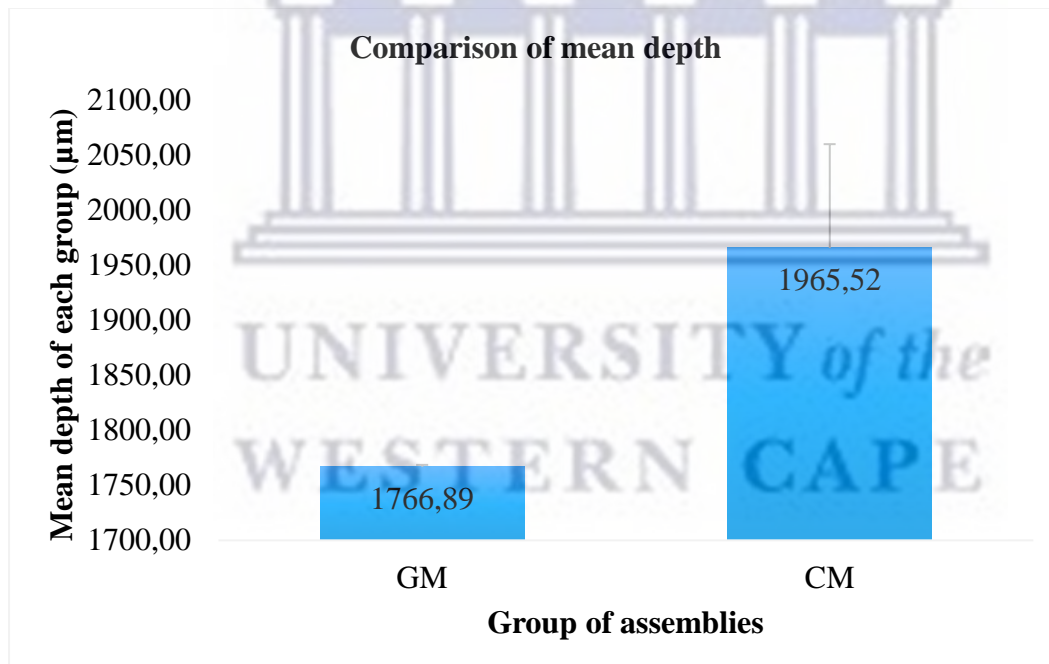


Figure 13: Graph illustrating the mean depth values of the IAI in Group 1 and 2.

Statistical data were mean values and standard deviations which underwent an independent t-test for comparison between the IAI length in the GM and CM groups. Figure 13 showed that the measurements were higher in the CM group, $(1965.52 \pm 421.531) \mu\text{m}$, while for the GM group, it was $(1766.89 \pm 7.301) \mu\text{m}$ (Table 8). Moreover, there were significant differences between both groups, $p = 0.049$. However, although there were statistical differences in the

length between the chosen equidistant points within the CM group more than within the GM group (Figure 14), there were no statistically significant differences within each group, $p=0.870$ for the GM group and $p=0.959$ for the CM group (Table 9).

Table 9: One Way Anova test used for comparison of variation in the means of depth and standard deviations within and across the GM and CM group.

ANOVA						
reading						
ASSEMBLY		Sum of Squares	df	Mean Square	F	Sig.
GM	Between Groups	45,293	3	15,098	0,236	0,870
	Within Groups	768,560	12	64,047		
	Total	813,853	15			
CM	Between Groups	67802,356	3	22600,785	0,100	0,959
	Within Groups	2715216,126	12	226268,011		
	Total	2783018,483	15			

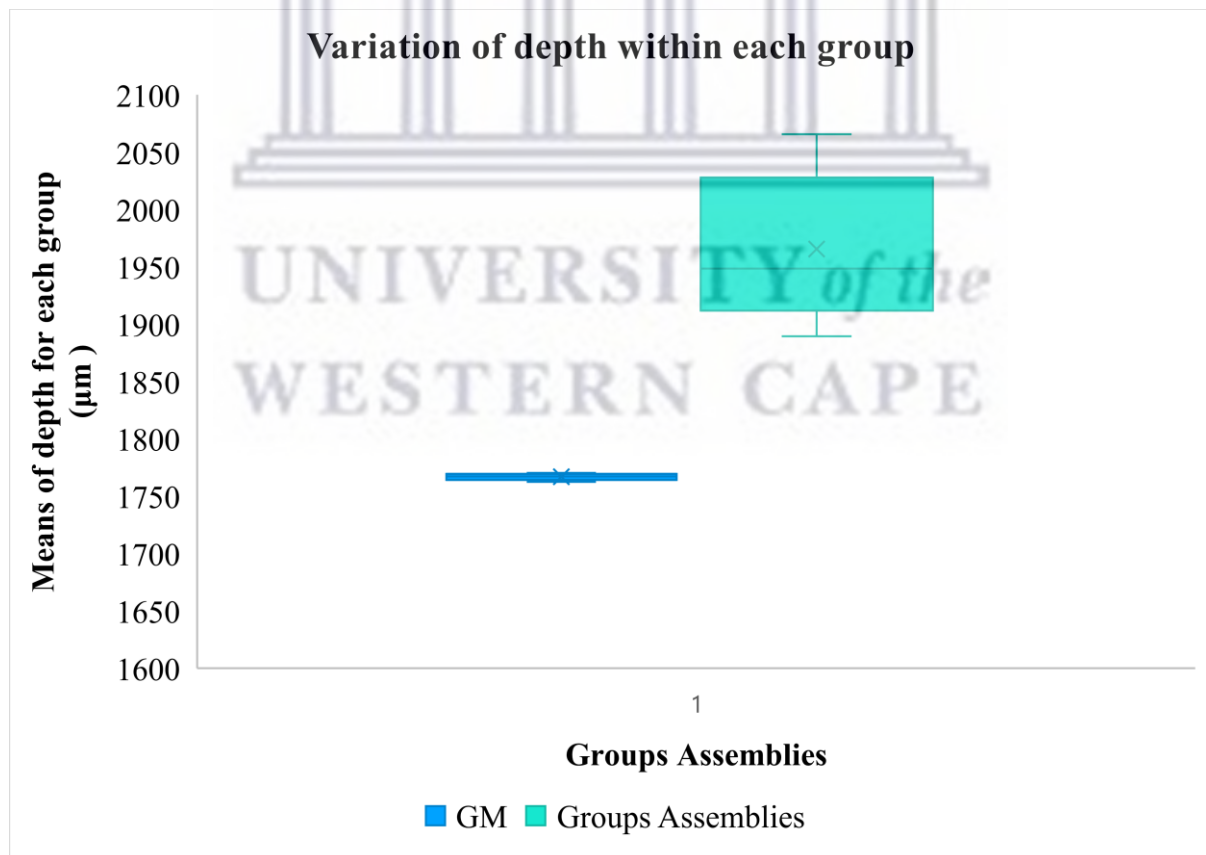


Figure 14: Graph illustrating the variations in the means of depth within and across the two groups.

CHAPTER 6: DISCUSSION

The use of dental implants as replacements for edentulous spaces has been reported as a highly successful and predictable procedure for many decades (Nascimento *et al.*, 2008). Nevertheless, prosthetic and biological factors can contribute to their occasional failure. It has been proposed that biological complications such as peri-implant marginal bone loss is a result of implant-abutment interface (IAI) microleakage in two stage implant systems (Scarano *et al.*, 2005). This microbial leakage can be attributed partially to the type and geometry of the implant- abutment connection (Ranieri *et al.*, 2015). Investigations reported that the connection's marginal fit, taper angle and the amount of torque used, play a determining role in the stability and subsequently the sealing ability of the conical implant system (Nassar & Abdalla, 2015; Ranieri *et al.*, 2015). Therefore, the aim of this present investigation was to determine the sealing capacity against microbial leakage of an implant with a novel conical (Morse taper) connection.

The *in vitro* bacterial analysis detected bacterial growth in both groups of implant assemblies. This result was consistent with a study conducted by Ranieri and his co-worker (2015) where four different groups of implants with internal conical (Morse taper) connection systems were submitted to bacterial culture resulting in different levels of bacterial colonization (Ranieri *et al.*, 2015). Aloise *et al.*'s study also showed similar results where two groups of Morse taper implant connections were tested and compared for sealing ability against leakage. Both groups showed variable amounts of bacterial leakage with no statistical significance (Aloise *et al.*, 2010). Likewise, in the present investigation there was no statistically significant difference between the two connections, although there was lower bacterial colonization in the GM connection showing contamination in only 20% of the tested specimens compared to 50% contamination in the CM connection. Koutouzis *et al.* detected statistically significant differences when using a larger sample size than in our study, to compare between bacterial leakage in Morse taper and conical grooved designs. Their study suggested that differences in connection designs can give variable results (Koutouzis *et al.*, 2011). Nevertheless, Dibert *et al.* reported that certain types of conical implants can provide hermetic sealing against bacterial leakage (Dibert *et al.*, 2005). Whether Morse taper implants can completely prevent microbial leakage or not, studies suggested that the mere presence of the implant abutment interface gap may result in peri-implant marginal bone loss (Ranieri *et al.*, 2015).

In the second part of the study, the SEM analysis revealed smaller micro-gap size in the CM connection (mean of 2.29 ± 0.26 μm compared to the GM connection (mean of 4.05 ± 0.45 μm).

μm . This would explain the bacterial leakage that occurred in some of the implant assemblies, since the average size of *S. sanguinis* is 0.5-1 μm which is smaller than the micro-gap size in both groups (da Silva-Neto *et al.*, 2012). However, this result could not explain the higher bacterial leakage detected in the CM connection with the narrower gap when compared to the GM connection in the bacterial analysis. The microbial leakage is possibly related to the size of the implant-abutment interface and marginal misfit (Nassar & Abdullah, 2015), although Jansen *et al.* (2010) reported a lack of correlation between the size of the micro-gap and the bacterial leakage in his study.

Moreover, another interesting result was associated with the degree of the taper angle in the two connections. The CM connection had a smaller taper angle (11.5°) when compared with the GM connection taper angle of 16° as provided by the manufacturer (Neodent® Implant Systems Inc., 2018). Studies concluded that the smaller the taper angle, the more cold welding and intimate contact between the implant and the abutment was created (Ranieri *et al.*, 2015). This conclusion was supported by Dibert *et al.*'s. (2005) study where a conical implant with 1.5° provided hermetic sealing against bacterial leakage. In the present investigation, there was higher bacterial penetration in implants with smaller taper angles and *vice versa*.

Albeit the exact reason for these contradictions was not clear, one possible explanation was the difference in the abutment screw torque between the two connections. In the GM connection the torque value used was 25 Ncm which was higher than the 15 Ncm used in the CM connection. The inverse relationship between the high torque value and the extent of bacterial leakage was documented previously (Ranieri *et al.*, 2015; Baggi *et al.*, 2013). Moreover, Smith and Turkyilmaz (2014) evaluated the effect of different screw torque values on the bacterial sealing ability of different implant-abutment connections. They reported that increasing the torque value over 20 Ncm resulted in less bacterial leakage in Zirconia abutments. However, Black *et al.* (2017) contradicted this result by reporting a lack of significant effect of the abutment type or of the increase in the screw torque value in creating a hermetic seal at the implant-abutment interface.

Another possible suggestion is the inconsistency in the length within the CM implant-abutment interface connection. The GM connection showed shorter length but with more regularity and consistency when compared to the CM connection in the micro CT scan analysis. Sasada and Cochran (2017) suggested that the longer the contact between the implant fixture and the abutment, the more stable the connection. This differs from the result

in the present investigation where more bacterial leakage occurred in the CM connection with the longer implant-abutment interface. A possible explanation for the difference is the variation in the right and left side depths of the CM connection (Figure 12:A) despite careful adaptation, precise torque application to the assemblies in the present investigation and the absence of contamination in the negative controls. However, we used one sample for depth investigation. Hence, a larger sample size would have been advisable because the difference in depths was not statistically significant in the CM connection.

The results of the current investigation agree with previous studies that reported the lack of hermetic sealing against microbial leakage, even in the conical (Morse taper) connection design (Aloise *et al.*, 2010; Koutouzis *et al.*, 2011; Teixeira *et al.*, 2011; Jaworski *et al.*, 2012; Nassar & Abdalla, 2015; Ranieri *et al.*, 2015). However, it is important to indicate that this study was the first laboratory analysis conducted to investigate the sealing capacity against bacterial leakage of the novel GM connection design.

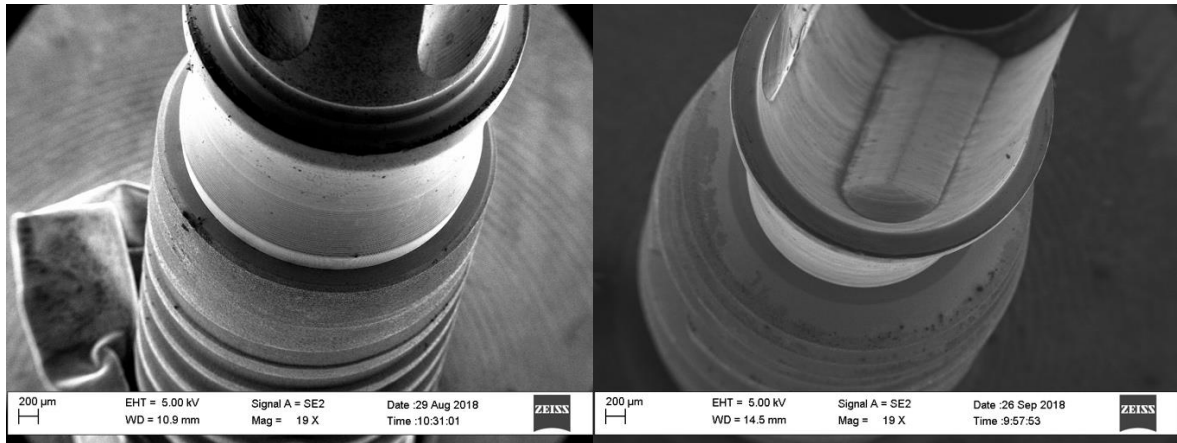


CHAPTER 7: LIMITATIONS

Even though the result of this current investigation was compatible with previous studies, certain shortcomings were encountered. One of the limitations was the use of a small sample size. Researchers found that using a limited sample size may lead to a large standard deviation compared to the mean value of a larger sample size, which results in more consistent data (Nawafleh *et al.*, 2013). Hence, to overcome this shortcoming, an increase in the number of measurements in the SEM and micro CT scanning was done. However, although implant assemblies could be sterilized and re-used to increase the sample size, this step was avoided in fear of the risk of abutment screw stripping and loss of the implant assembly.

Another limitation that arose in this study occurred during the SEM image production. The geometry of the conical connection made it impossible to view the interface at a right angle to the long axis of the assembly nor straight from above. Therefore, an attempt was made to cut the abutment head off. However, this resulted in loss of the torque force and loosening of the implant-abutment connection. Therefore, the implant-abutment interface outer side was viewed from above with tilting the assembly to an angle that exposed the gap (Figure 15). For both groups' corresponding abutments, the narrow width of the conical abutment allowed for implant-abutment interface viewing. However, the reproduction of the exact angle for all the assemblies was not possible, which could have led to variation in the results.

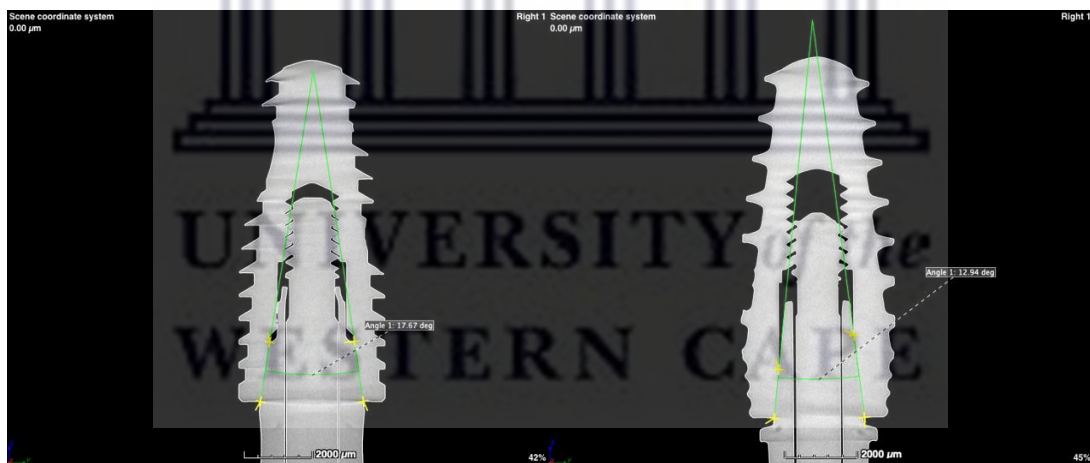
Likewise, the use of micro CT scanning for measuring the taper angle of the IAI in both connections was limited due to the lack of fixed points on the assembly to use as a reference point for correct angle calculation at different axes and magnification powers (Figure 16). However, the connection taper angles were obtained from the implant manufacturer's catalogue as 16° for a GM connection and 11.5° for a CM connection (Neodent® Implant Systems Inc., 2018).



A

B

Figure 15: The tilting angle of the implant assembly to view the IAI via SEM. A- GM connection assembly using SEM image. B- CM connection assembly (magnification of x19).



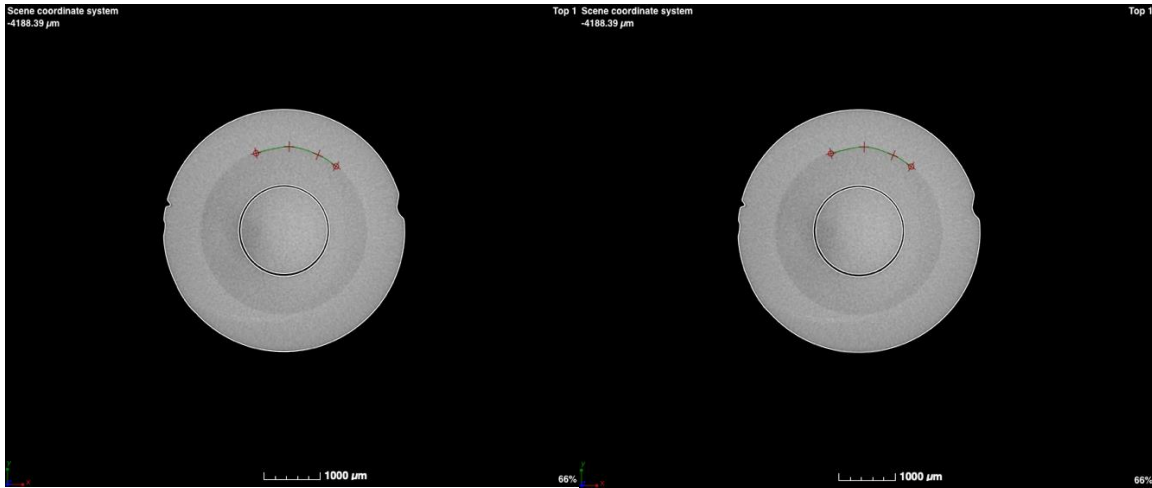
A

B

Figure 16: Measuring the angle of the IAI at the y-z plane. A- GM connection assembly using SEM image. B- CM connection assembly (magnification of x2000 µm).

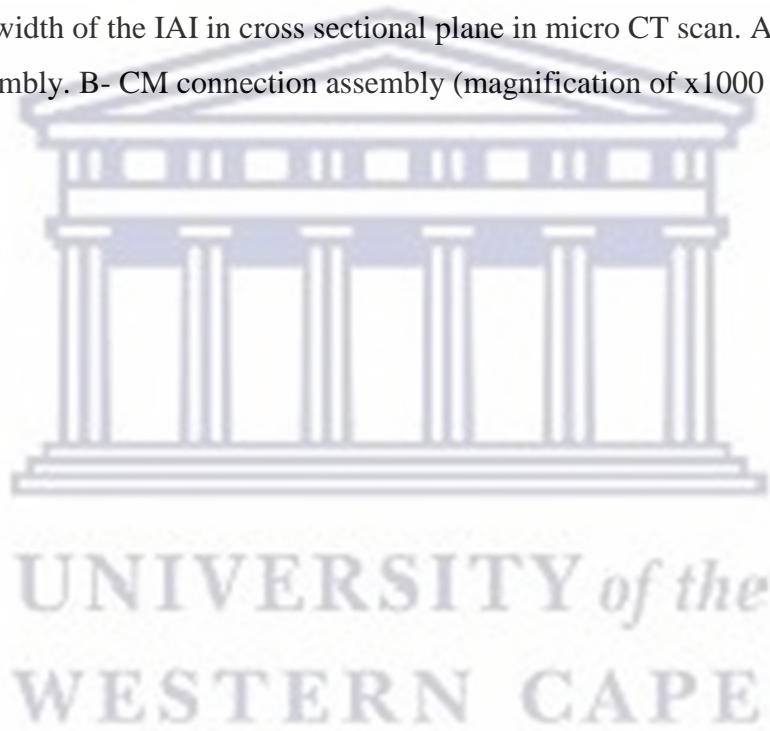
Another limitation in this study was the inability to measure the implant-abutment interface micro-gap size, using the micro CT scan. This was intended to be a confirmation step to the micro-gap size already obtained from the SEM analysis but the maximum magnification that could be viewed was limited to 10 μm (Figure 17). Hence, the produced image could not view the interface between the implant and the abutment to perform the measurement. Studies reported that the micro-gap size in the conical internal connection design was an average of $6.61 \pm 3.17 \mu\text{m}$ which was confirmed by the SEM analysis to be less than 10 μm in both groups (Ranieri *et al.*, 2015).

In spite of all these limitations, the result of the current investigation agrees with previous studies that reported the lack of hermetic sealing against microbial leakage even in the conical (Morse taper) connection design (Aloise *et al.*, 2010; Koutouzis *et al.*, 2011; Teixeira *et al.*, 2011; Jaworski *et al.*, 2012; Nassar & Abdalla, 2015; Ranieri *et al.*, 2015). Although no statistical relation was evident, the unique features of the novel implant system might add some advantageous input in the microbial sealing, resulting in less microbial leakage and more uniform design. This result could suggest the need for a larger sample size to increase the confidence level in the novel connection investigation. It is important to point out that this study was the first laboratory analysis conducted to investigate the sealing capacity against bacterial leakage of the novel GM connection design. It would be fair to state that bacterial leakage evaluation in this model of association requires further investigation with a larger sample size in addition to long term *in vivo* and *in vitro* studies. Moreover, it would be interesting to evaluate the novel connection design's prosthetic features such as stability under load and the effect on bacterial sealing capacity in future investigations.



B

Figure 17: The width of the IAI in cross sectional plane in micro CT scan. A-GM connection assembly. B- CM connection assembly (magnification of $\times 1000 \mu\text{m}$).



CHAPTER 8: CONCLUSION

Based on the study design, and considering the previously mentioned limitations, no significant statistical differences were found between the two implant abutment designs. Theoretically, the clinician can apply any implant connection design from the two systems under investigation, when it comes to the sealing capacity against bacterial leakage. Whether the novel connection design has an effect on the prosthetic complications was not within the scope of the study and further research is required to investigate this aspect.



REFERENCES

- Almeida, E. O. *et al.* (2013) 'Mechanical testing of implant-supported anterior crowns with different implant/abutment connections.', *International Journal of Oral & Maxillofacial Implants*, 28(1).
- Aloise, J. P. *et al.* (2010) 'Microbial leakage through the implant–abutment interface of Morse taper implants *in vitro*', *Clinical oral implants research*, 21(3), pp. 328–335.
- Baggi, L. *et al.* (2013) 'Microbiological evaluation of bacterial and mycotic seal in implant systems with different implant-abutment interfaces and closing torque values', *Implant dentistry*, 22(4), pp. 344–350.
- Barbosa, R. E. S. *et al.* (2009) 'Bacterial culture and DNA Checkerboard for the detection of internal contamination in dental implants', *Journal of Prosthodontics*, 18(5), pp. 376–381.
- Binon, P. P. (2000) 'Implants and components: entering the new millennium.', *The International journal of oral & maxillofacial implants*, 15(1), p. 76.
- Black, D. L. *et al.* (2017) 'Evaluation of the Sealing Capability of the Internal Conical Connections of Implants with Titanium and Zirconia Abutments.', *The journal of contemporary dental practice*, 18(10), pp. 915–922.
- Branemark, P. I. (1977) 'Osseointegrated implants in the treatment of edentulous jaw, Experience from a 10-year period', *Scand J Plast Reconstr Surg*, 1, pp. 1–132.
- Broggini, N. *et al.* (2003) 'Persistent acute inflammation at the implant-abutment interface', *Journal of dental research*, 82(3), pp. 232–237.
- Canullo, L. *et al.* (2015) 'Microbiological assessment of the implant-abutment interface in different connections: cross-sectional study after 5 years of functional loading', *Clinical oral implants research*, 26(4), pp. 426–434.
- Coelho, P. G. *et al.* (2008) '*In vitro* evaluation of the implant abutment connection sealing capability of different implant systems', *Journal of oral rehabilitation*, 35(12), pp. 917–924.
- Coppede, A. R. *et al.* (2009) 'Fracture resistance of the implant-abutment connection in implants with internal hex and internal conical connections under oblique compressive

loading: an *in vitro* study.’, *International Journal of Prosthodontics*, 22(3).

Costa, G. N. *et al.* (2017) ‘Microbiological Sealing Analysis of a Tapered Connection and External Hexagon System’, *International journal of dentistry*, 2017.

Dias, E. C. L. de C. *et al.* (2012) ‘Evaluation of implant-abutment microgap and bacterial leakage in five external-hex implant systems: an *in vitro* study.’, *International Journal of Oral & Maxillofacial Implants*, 27(2).

Dibart, S. *et al.* (2005) ‘*In vitro* evaluation of the implant-abutment bacterial seal: the locking taper system.’, *International Journal of Oral & Maxillofacial Implants*, 20(5).

Ding Thomas A., W. R. D. H. F. L. M. B. H. (2003) ‘Evaluation of the ITI Morse Taper Implant/ Abutment Design with an Internal Modification’, *The International Journal of Oral & Maxillofacial Implants*, Volume 18(Issue 6), pp. 865–872.

Ericsson, I. *et al.* (1996) ‘The effect of antimicrobial theram on peri-implantitis lesions. An experimental study in the dog.’, *Clinical oral implants research*, 7(4), pp. 320–328.

De Faria, K. O. *et al.* (2013) ‘Comparison of methods to evaluate implant-abutment interface’, *Brazilian Journal of Oral Sciences*, 12(1), pp. 37–40.

Garrana, R. *et al.* (2016) ‘Leakage of Microbial Endotoxin through the Implant-Abutment Interface in Oral Implants: An *In vitro* Study’, *BioMed Research International*, 2016, p. 6.

Goiato, M. C. *et al.* (2015) ‘Is the internal connection more efficient than external connection in mechanical, biological, and esthetical point of views? A systematic review’, *Oral and maxillofacial surgery*, 19(3), pp. 229–242.

Harder, S. *et al.* (2010) ‘Molecular leakage at implant-abutment connection—*in vitro* investigation of tightness of internal conical implant-abutment connections against endotoxin penetration’, *Clinical oral investigations*, 14(4), pp. 427–432.

Jansen, V. K., Conrads, G. and Richter, E.-J. (1997) ‘Microbial leakage and marginal fit of the implant-abutment interface.’, *International Journal of Oral & Maxillofacial Implants*, 12(4).

Jansen, V. K., Conrads, G. and Richter, E.-J. (1997) ‘Microbial leakage and marginal fit of

the implant-abutment interface.’, *International Journal of Oral & Maxillofacial Implants*, 12(4).

Jaworski, M. E. *et al.* (2012) ‘Analysis of the bacterial seal at the implant-abutment interface in external-hexagon and Morse taper-connection implants: an *in vitro* study using a new methodology.’, *International Journal of Oral & Maxillofacial Implants*, 27(5).

Koutouzis, T. *et al.* (2011) ‘Bacterial colonization of the implant–abutment interface using an *in vitro* dynamic loading model’, *Journal of periodontology*, 82(4), pp. 613–618.

Muley, N., Prithviraj, D. R. and Gupta, V. (2012) ‘Evolution of external and internal implant to abutment connection’, *Int J Oral Implantol Clin Res*, 3(3), pp. 122–129.

Do Nascimento, C. *et al.* (2011) ‘*In vitro* evaluation of bacterial leakage along the implant-abutment interface of an external-hex implant after saliva incubation’, *International Journal of Oral and Maxillofacial Implants*, 26(4), p. 782.

Nascimento, C. Do *et al.* (2008) ‘Bacterial leakage along the implant–abutment interface of premachined or cast components’, *International journal of oral and maxillofacial surgery*, 37(2), pp. 177–180.

Nascimento, C. Do, Pedrazzi, V., *et al.* (2009a) ‘Influence of repeated screw tightening on bacterial leakage along the implant–abutment interface’, *Clinical oral implants research*, 20(12), pp. 1394–1397.

Nascimento, C. Do, Barbosa, R. E. S., *et al.* (2009b) ‘Use of checkerboard DNA–DNA hybridization to evaluate the internal contamination of dental implants and comparison of bacterial leakage with cast or pre-machined abutments’, *Clinical oral implants research*, 20(6), pp. 571–577.

Do Nascimento, D. M. D. C. *et al.* (2012) ‘Leakage of saliva through the implant-abutment interface: *in vitro* evaluation of three different implant connections under unloaded and loaded conditions’, *The International journal of oral & maxillofacial implants*, 27(3).

Nassar, H. I. and Abdalla, M. F. (2015) ‘Bacterial leakage of different internal implant/abutment connection’, *Future Dental Journal*, 1(1), pp. 1–5.

Nawafleh, N. A. *et al.* (2013) ‘Accuracy and reliability of methods to measure marginal

adaptation of crowns and FDPs: a literature review’, *Journal of Prosthodontics*, 22(5), pp. 419–428.

Neodent® Implant Systems Inc. (2018) *NEODENT® GRAND MORSE™ IMPLANT SYSTEM*. Available at: <https://www.straumann.com/neodent/fi/en/discover/grand-morse.html> (Accessed: 16 April 2019).

De Oliveira, G. R. *et al.* (2014) ‘Bacterial contamination along implant-abutment interface in external and internal-hex dental implants’, *International Journal of Clinical and Experimental Medicine*, 7(3), pp. 580–585.

Peñarrocha-Diago, M. A. *et al.* (2013) ‘Influence of implant neck design and implant–abutment connection type on peri-implant health. Radiological study’, *Clinical oral implants research*, 24(11), pp. 1192–1200.

Persson, L. G. *et al.* (1996) ‘Bacterial colonization on internal surfaces of Brånemark system® implant components’, *Clinical oral implants research*, 7(2), pp. 90–95.

Ranieri, R. *et al.* (2015) ‘The Bacterial Sealing Capacity of Morse Taper Implant–Abutment Systems *in vitro*’, *Journal of periodontology*, 86(5), pp. 696–702.

Rismanchian Mansoor. Hatami., M. B. H. K. N. G. H. (2012) ‘Evaluation of Microgap Size and Microbial Leakage in the Connection Area of 4 Abutments With Straumann (ITI) Implant.’, *Journal of Oral Implantology*, Vol. 38(Issue 6), pp. 677–685.

Ronald, R. A., Micheal, B. and Joseph, J. G. (1980) ‘Bactericidal Activity of Human Lactoferrin: Sensitivity of a Variety of Microorganisms’, *Infection and immunity*, pp. 893–898.

Sasada, Y. and Cochran, D. L. (2017) ‘Implant-Abutment Connections: A Review of Biologic Consequences and Peri-implantitis Implications.’, *International Journal of Oral & Maxillofacial Implants*, 32(6).

Scarano, A. *et al.* (2005) ‘A 16–year Study of the Microgap Between 272 Human Titanium Implants and Their Abutments’, *Journal of Oral Implantology*, 31(6), pp. 269–275.

Shafie and Hamid, R. (2014) *Clinical and Laboratory Manual of Dental Implant Abutments*. John Wiley & Sons.

Da Silva-Neto, J. P. *et al.* (2012) 'Influence of methodologic aspects on the results of implant-abutment interface microleakage tests: a critical review of *in vitro* studies.', *International Journal of Oral & Maxillofacial Implants*, 27(4).

Smith, N. A. and Turkyilmaz, I. (2014) 'Evaluation of the sealing capability of implants to titanium and zirconia abutments against *Porphyromonas gingivalis*, *Prevotella intermedia*, and *Fusobacterium nucleatum* under different screw torque values', *The Journal of prosthetic dentistry*, 112(3), pp. 561–567.

Steinebrunner, L. *et al.* (2005) 'In vitro evaluation of bacterial leakage along the implant-abutment interface of different implant systems.', *International Journal of Oral & Maxillofacial Implants*, 20(6).

Sutton, S. (2011) 'Accuracy of plate counts', *Journal of validation technology*, 17(3), pp. 42–46.

Teixeira, W. *et al.* (2011) 'Microleakage into and from two-stage implants: an *in vitro* comparative study.', *International Journal of Oral & Maxillofacial Implants*, 26(1).

Wachtel, A. *et al.* (2016) 'A Novel Approach to Prove Bacterial Leakage of Implant-Abutment Connections *In vitro*', *Journal of Oral Implantology*, 42(6), pp. 452–457.

Yip, G., Schneider, P. and Roberts, E. W. (2004) 'Micro-computed tomography: high resolution imaging of bone and implants in three dimensions', in *Seminars in Orthodontics*. Elsevier, pp. 174–187.

APPENDIXES

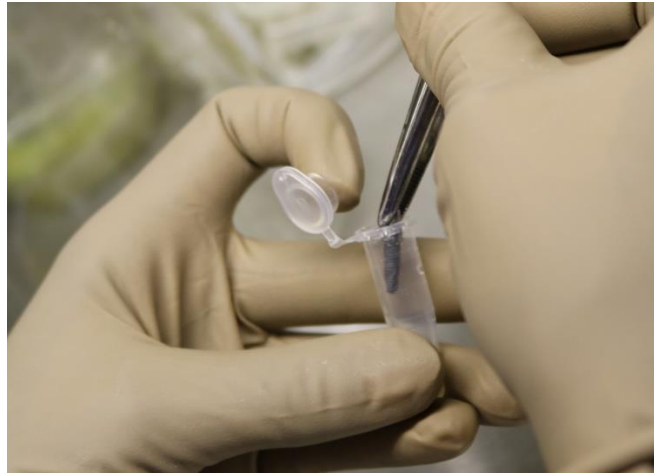
Appendix A: Methodology



Figure 1: An implant connected to the corresponding abutment using the torque wrench according to the manufacturer's instructions.



Figure 2: An implant assembly submerged in BHI above the IAI level and below the screw hole.



A



B

Figure 3: A-Implant assembly removed from the test tubes using sterile pliers. B- Placed vertically in a stand for drying.



Figure 4: The implant's inner surface was sampled by sterile paper points for bacterial contamination.

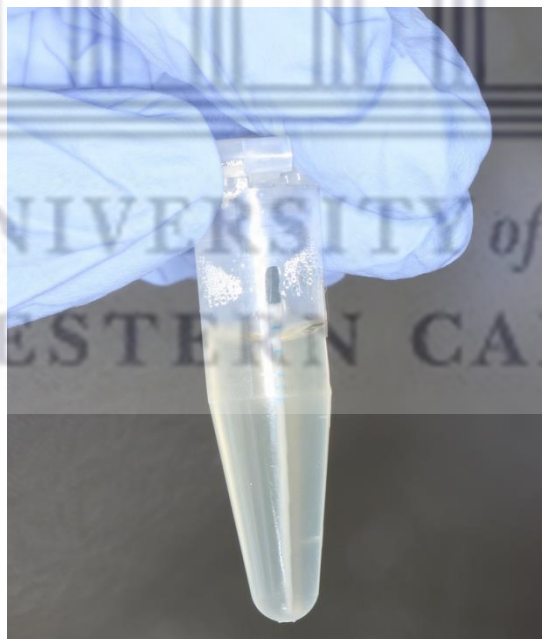


Figure 5: Immersion of paper points in test tubes containing sterile BHI broth for 20 minutes.

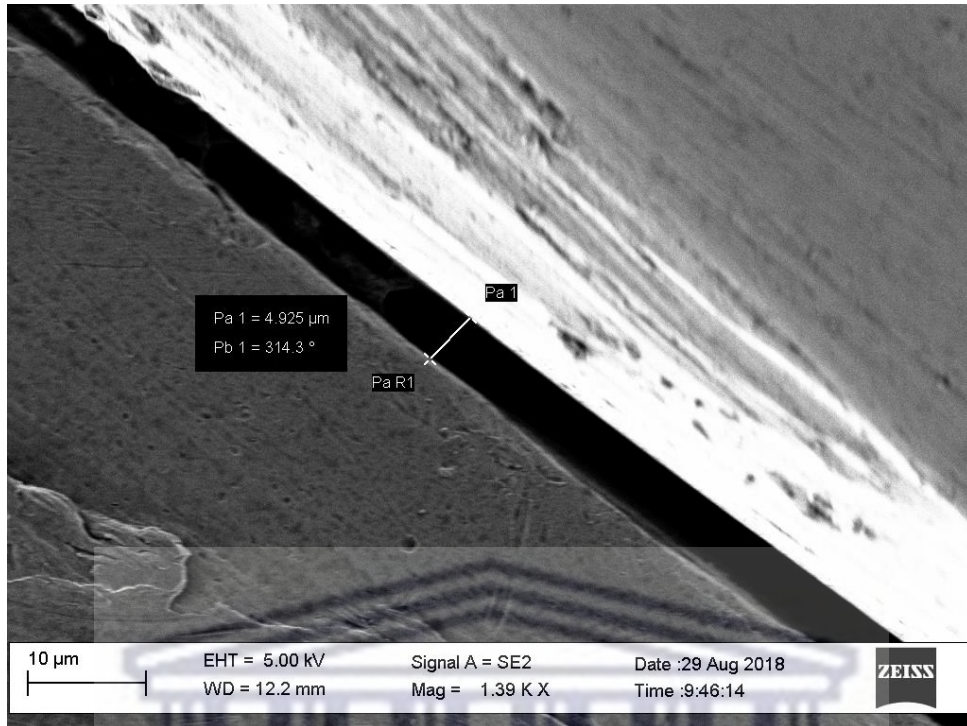


Figure 6: Measurement of the interface at a random point in implant assembly from GM group (magnification of x1.39k).

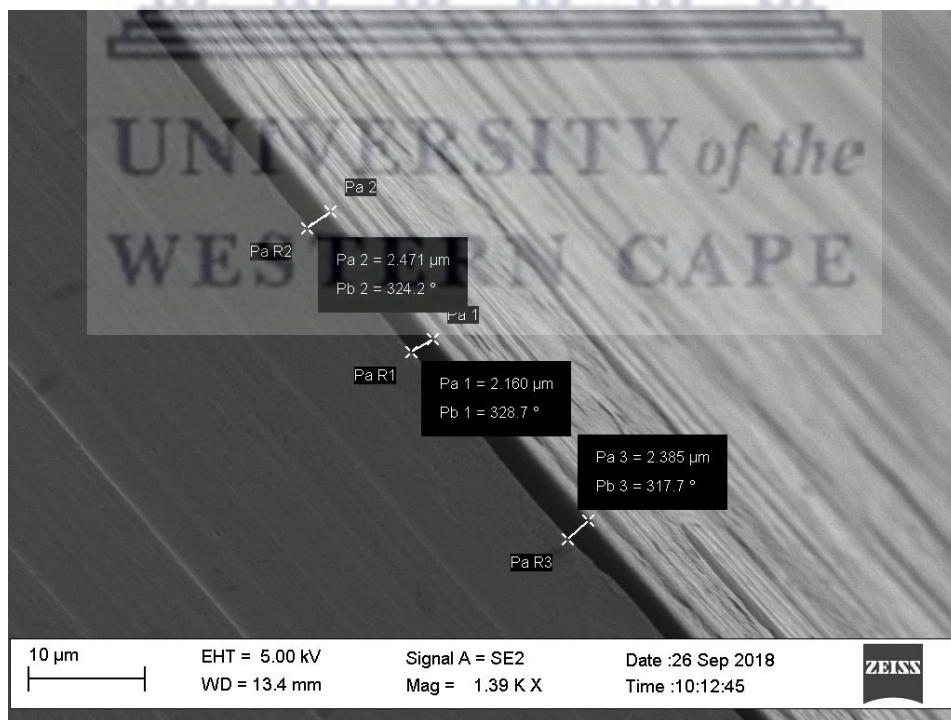
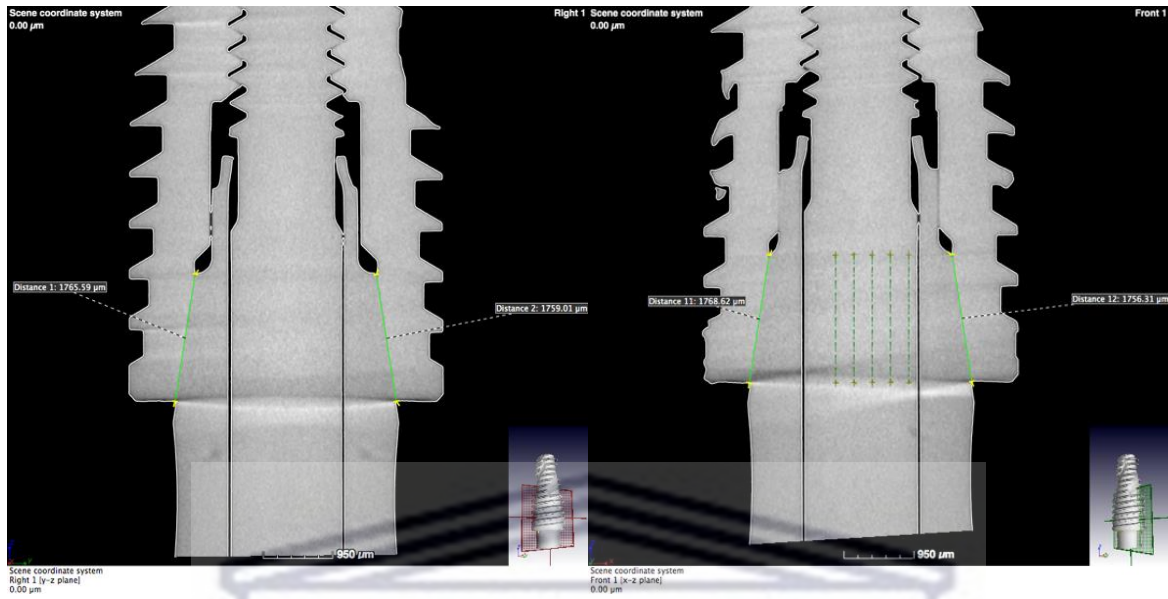


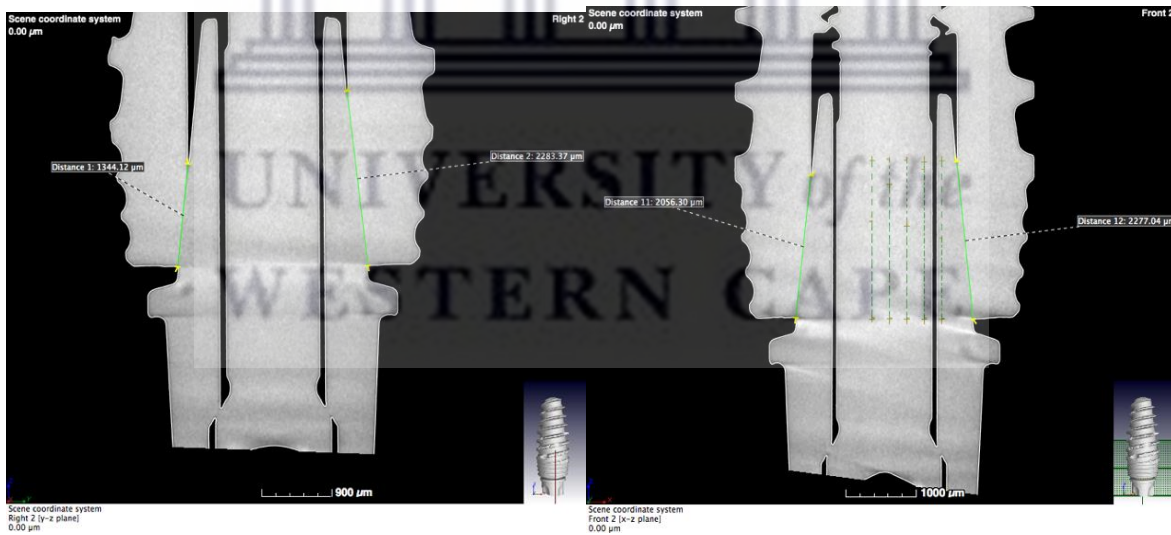
Figure 7: Measurement of the interface at random points in implant assembly from CM group (magnification of x1.39k).



A

B

Figure 8: The depth of the IAI on the left and right sides of the GM connection. A- At 0.00 μm point on the y-z plane. B- At 0.00 μm point on the x-z plane (magnification of x950 μm).



A

B

Figure 9: Measurement of the depth of the IAI on the left and right sides of the CM connection A- At 0.00 μm point on the y-z plane. B- At 0.00 μm point on the x-z plane (magnification of x900 μm).

Appendix B: Data Collection Tables

Table 1: Data collection in the bacterial leakage analysis of GM connection assemblies.

Assembly	Inoculation date	Extraction date	Data collection date	Results	CFU
GM1	25.6.2018	27.6.2018	28.6.2018	no growth	
GM2	25.6.2018	27.6.2018	28.6.2018	no growth	
GM3	25.6.2018	27.6.2018	28.6.2018	no growth	
GM4	25.6.2018	27.6.2018	28.6.2018	no growth	
GM5	25.6.2018	27.6.2018	28.6.2018	no growth	
GM6	25.6.2018	27.6.2018	28.6.2018	no growth	
GM7	25.6.2018	27.6.2018	28.6.2018	bacterial growth	252 colonies
GM8	25.6.2018	27.6.2018	28.6.2018	no growth	
GM9	25.6.2018	27.6.2018	28.6.2018	no growth	
GM10	25.6.2018	27.6.2018	28.6.2018	bacterial growth	>300 colonies
BHI negative control	25.6.2018	27.6.2018	28.6.2018	no growth	

Table 2: Data collection in the bacterial leakage analysis of CM connection assemblies.

Assembly	Inoculation date	Extraction date	Data collection date	Results	CFU
CM1	26.6.2018	28.6.2018	29.6.2018	no growth	
CM2	26.6.2018	28.6.2018	29.6.2018	no growth	
CM3	26.6.2018	28.6.2018	29.6.2018	no growth	
CM4	26.6.2018	28.6.2018	29.6.2018	bacterial growth	103 colonies
CM5	26.6.2018	28.6.2018	29.6.2018	bacterial growth	>300 colonies
CM6	26.6.2018	28.6.2018	29.6.2018	bacterial growth	30 colonies
CM7	26.6.2018	28.6.2018	29.6.2018	bacterial growth	>300 colonies
CM8	26.6.2018	28.6.2018	29.6.2018	no growth	
CM9	26.6.2018	28.6.2018	29.6.2018	no growth	
CM10	26.6.2018	28.6.2018	29.6.2018	bacterial growth	235 colonies
BHI negative control 2	26.6.2018	28.6.2018	29.6.2018	no growth	

Table 3: The GM connection assemblies measurement of IAI width using SEM analysis.

Readings	IAI Width (Sample 1) µm	IAI Width (Sample 2) µm
reading 1	3,463	4,370
reading 2	4,088	4,925
reading 3	3,969	4,190
reading 4	3,562	4,256
reading 5	3,887	4,541
reading 6	3,551	4,748
reading 7	3,450	4,231
reading 8	3,297	3,438
reading 9	3,982	3,844
reading 10	4,299	3,841
reading 11	4,458	4,376
reading 12	4,656	3,771

UNIVERSITY of the
WESTERN CAPE

Table 4: The CM connection assemblies measurement of IAI width using SEM analysis.

Readings	IAI Width (Sample 1) µm	IAI Width (Sample 2) µm
reading 1	2,471	1,541
reading 2	2,160	2,099
reading 3	2,385	2,358
reading 4	2,234	2,475
reading 5	2,549	2,594
reading 6	2,229	1,878
reading 7	2,338	2,147
reading 8	2,189	2,404
reading 9	2,264	2,459
reading 10	2,294	2,906
reading 11	2,359	2,282
reading 12	2,134	2,325

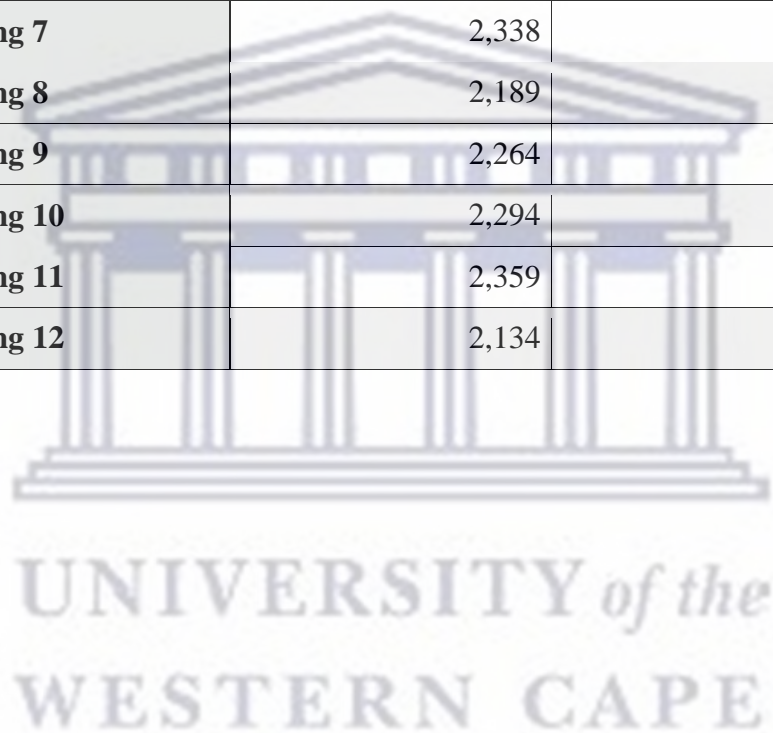


Table 5: The GM group measurements of IAI depth on the y-z and x-z axes at different equidistant points.

The scene coordinate system points	y-z axis		x-z axis	
	GM reading 1(μm) Left	GM reading 2(μm) Right	GM reading 1 (μm) Left	GM reading 2 (μm) Right
0.00um	1765.59	1759.01	1768.62	1756.31
250um	1769.19	1765.55	1770.31	1764.13
-250um	1774.72	1782.96	1768.12	1755.25
500um	1778.14	1761.66	1774.74	1760.47
-500um	1770.73	1767.16	1767.06	1757.98

Table 6: The CM group measurement of IAI depth on the y-z and x-z axes at different equidistant points.

The scene coordinate system points	y-z axis		x-z axis	
	CM reading 1(μm) Left	CM reading 2 (μm) Right	CM reading 1 (μm) Left	CM reading 2 (μm) Right
0.00um	1344.12 um	2283.37	2056.30	2277.04
250um	2272.24	2156.83	1087.60	2276.70
-250um	1940.44	2295.69	2282.21	1744.23
500um	2295.69	1169.10	2286.40	1984.57
-500um	2290.34	1398.75	2288.74	1579.98

UNIVERSITY of the
WESTERN CAPE

APPENDIX C: Ethical Approval.



OFFICE OF THE DIRECTOR: RESEARCH RESEARCH AND INNOVATION DIVISION

Private Bag X17, Bellville 7535
South Africa
T: +27 21 959 4111/2948
F: +27 21 959 3170
E: research-ethics@uwc.ac.za
www.uwc.ac.za

6 February 2019

Dr S Kabbashi
Faculty of Dentistry

Ethics Reference Number: BM18/1/4

Project Title: An in vitro study of bacterial leakage of a novel implant-abutment interface.

Approval Period: 23 February 2018 – 23 February 2019

I hereby certify that the Biomedical Science Research Ethics Committee of the University of the Western Cape approved the scientific methodology and ethics of the above mentioned research project.

Any amendments, extension or other modifications to the protocol must be submitted to the Ethics Committee for approval.

Please remember to submit a progress report in good time for annual renewal.

The Committee must be informed of any serious adverse event and/or termination of the study.

A handwritten signature in black ink, appearing to read 'Josias'.

*Ms Patricia Josias
Research Ethics Committee Officer
University of the Western Cape*

BMREC REGISTRATION NUMBER -130416-050